NEURAL RESPONSES TO INJURY: PREVENTION, PROTECTION, AND REPAIR
Annual Technical Report
1996-1997

Submitted by

Nicolas G. Bazan, M.D., Ph.D.
Project Director

Period Covered: 20 September, 1996 through 19 September, 1997

Cooperative Agreement DAMD17-93-V-3013

between

United States Army Medical Research and Development Command
(Walter Reed Army Institute of Research)

and

Louisiana State University Medical Center
Neuroscience Center of Excellence

Volume 8 of 9

Vision, Laser Eye Injury, and Infectious Diseases

Project Directors:
Herbert E. Kaufman, M.D.
Roger W. Beuerman, Ph.D.

Chapter 9, VISION, LASER EYE INJURY, AND INFECTIOUS DISEASES

PROGRAM DIRECTORS: Herbert E. Kaufman, M.D.
Roger W. Beuerman, Ph.D.

PARTICIPATING SCIENTISTS: Claude A. Burgoyne, M.D.
Emily D. Varnell
Mandi Conway, M.D.

I. INTRODUCTION

Four specific aims were proposed in the original grant application

A. Develop a new confocal microscope that can be used in living eyes to understand the earliest stages of trauma, laser injuries, and disease. We believed that a compact, portable confocal microscope could be developed that will replace the slit lamp biomicroscope and ophthalmoscopes which are used in routine ophthalmic exams, and which will provide much more needed information about laser damage, trauma, and other diseases in soldiers.

B. Evaluate drugs to prevent retinal damage after laser injury. The pathogenesis of damage by trauma and laser is poorly understood. Pain and damage can disable people hours after injury, and being able to assess damage immediately will permit the appropriate assignment of personnel and aid in the prediction of subsequent disability. We proposed to use the confocal microscope to study eye damage after laser injury and to evaluate drugs such of calcium channel blockers, glutamate inhibitors, and PAF inhibitors for their effects on preventing and treating laser damaged tissue.

C. Study traumatic and non-traumatic glaucoma to determine its pathogenesis. Glaucoma occurs as the result of trauma, as well as the result of an inherited condition. We proposed to use the confocal microscope to determine whether the outflow of fluid inside the eye has been changed, and to follow changes in the optic nerve, retinal vessels, nerve fiber layers, and in the ganglion cells.

D. Study drugs that will prevent the recurrence ocular herpes. Approximately 80% of adults have been infected with herpes virus, and 20 - 25% of these will develop

clinical disease in the form of cold sores, sun poisoning, or ocular disease. The ocular disease causes extreme morbidity and blindness. Recurrences of herpes are more common in times of stress, and the effective prevention of recurrences would be of critical importance.

GENERAL STATUS REPORT

We have made solid achievements in developing a small, compact, portable confocal microscope for examination of the cornea. With some additional development this microscope will also permit the detailed cellular examination of skin and retina. We expect that it will be usable for the early detection of vesicants and irritants to the skin and cornea, and that the precise cellular documentation of early damage can give a prognosis for how disabled a soldier will be at later times. Similarly, we think that adapting this to the retina will permit similar early detection of laser injury and, more important, an appraisal of future disability. The ability to diagnose both infectious and chemical damage of the cornea, skin, and retina at an early stage with enough visual detail with a light, rugged instrument usable by a corpsman could be a very significant benefit to the Army. We hope that we will be able to continue this development.

II. STUDIES AND RESULTS

A. Study a new confocal microscope that can be used in living eyes to understand the earliest stages of trauma, laser injuries, and disease

During our first year of study, we were able, for the first time to make cellular

observations in the living eye following injury. We found that laser injury to the cornea is first recognizable as an increase in the refractile properties of the nuclei of the cells immediately beneath the injury site. This response, which appears within hours, occurs in the cells that eventually become fibroblastic. Thus, the nuclear changes may be the earliest predictor of the fibroblastic response. These studies constitute one phase of the confocal project, which focused on optimizing the optics of the instrument and developing a new mechanical mount that can be used with human as well as animal subjects. Design changes increased the available light and improved image contrast. Observation of human eyes in vivo showed that this confocal microscope can be used on an "as needed" basis and that scanning through the depths of the tissues is rapid and without undue stress to the subject. Animal studies showed that the confocal microscope can be used to repeatedly return to a particular site within the eye in order to follow changes over several weeks. Increased light scattering in ocular tissues or media, as may occur after injury, often limits the type of information that can be obtained using current diagnostic tools such as the slit lamp biomicroscope. With the confocal microscope, however, objective information concerning infectious and inflammatory events at the cellular level may be easily obtained to facilitate real-time, non-invasive diagnosis of clinical ocular disease. We made substantial design changes both to the optics of the real-time confocal microscope and to its mechanical support for human and animal research.

In the second year of our studies, we reported that we were able to obtain images of the endothelial layer of the cornea in human subjects. This monolayer of cells is the most important in maintaining normal corneal thickness and transparency.

Confocal examination revealed the endothelial white bodies organized into a generally hexagonal arrangement, Cells formed a continuous mosaic with dark, often unclear borders between cells. A process was developed using image analysis employing digital filtering techniques and morphological operations to accurately determine the size and location of each cell. We also reported that improvements permitted the identification in patients of infectious organisms, fungus, bacteria, and *Acanthamoeba*. This identification could be carried out in 3 to 5 minutes and treatment could be initiated immediately. This instrument was also modified to be more rugged, and should make it possible to move the confocal microscope into positions for immediate determination of treatment for injured military personnel. Additional modifications allowed us to incorporate immunofluorescence capabilities to the microscope. Animal studies proved that it was possible to utilize the confocal microscope in conjunction with fluorescein-labeled antibody to herpes virus and to visualize virus infected cells.

In the third year of our studies, we reported that we were able to produce full-thickness, three-dimensional reconstruction from multiple optical sections of the normal in vivo human cornea. This allowed visualization of structures that were not apparent in conventional optical sections or in single confocal sections because of limited density of the object. We also reported that a much smaller, rugged microscope was produced which is 4 inched by 4 inched by 6 inched long. The optical design is also stable and daily adjustments are unnecessary,

The confocal microscope discussed and used in the previous year's report, consisted of a single-sided disk-type design. This design permits the microscope to operate with a minimum number of mirrors. This factor is desirable since mirrors

introduce the unwanted possible effects of misalignment, degraded image from surface debris, and degradation of the mirrored surface. Additionally, the single-sided disk-design avoids any disk alignment difficulties since the same set of pinholes are used in both directions of the light path. The body of this microscope was approximately rectangular with a height and width of 18 cm and a body length of 40 cm.

During the use of the single-sided disk confocal microscope, it became apparent that image contrast and illumination were decreasing. Examination of the microscope revealed that the semi-silvered mirror which reflects the illuminating light forward, toward the objective, had decreased reflectivity and greater transmission of the light through the semi-silvered mirror. The mirror was removed and the transmission of the light, which should have been 50%, was measured. The transmission was found to be 80% in the central portion of the mirror. The increased transmission of light through the mirror was found to decrease contrast and image brightness by reducing the amount of light which reached the specimen, and permitting an increased amount of light which was reflected by the solid surface of the single-sided disk to reach the camera sensor. We speculate that the high energy photons from the 300 watt xenon arc removed the semi-silver coating in the central portion of this integral mirror.

Although the mirror could easily be replaced, a permanent solution to this serious problem was sought. Technological advances and decreased costs of supplies permitted the construction of a new confocal microscope of the tandem scanning design. Our new confocal microscope incorporates many practical design modificationist. Specifically, the semi-silvered mirror is placed posterior to the disk in the light path. This protects the mirror from direct exposure to the high energy photons

which were thought to have damaged the mirror in the previous single-sided disk design. Secondly, the diameter of the Nipkow disk was reduced in size. Third, we designed a very stable mounting system for the disk which requires only an initial alignment and no further adjustments after the manufacture of the confocal microscope "box". Thus, these advances permitted a confocal microscope which is a cube measuring roughly 12 cm per side. This marked reduction in size reduces manufacturing costs of the microscope, increases the manuervability and useability of the confocal microscope, and increases the potential for true portable use of the microscope.

A new objective for the microscope was obtained which permitted the examination depth to increase from .65 mm to 1.5 mm through the specimen. Furthermore, the objective posseses a higher numerical aperture (NA), which provides a brighter, higher contrast, high resolution image.

1. Corneal damage after exposure to ultra-violet and short wave length lasers and ultraviolet light

During the first year of this grant, we studied the effects of an excimer laser which is a 193 nm argon-fluoride laser used to remove tissue from the anterior corneal stroma. A major postoperative response has been the development of a subepithelial fibrotic haze, which has been seen in all animals including primates and humans. We used the confocal microscope to investigate the cellular level corneal changes in vivo during the first week after excimer laser ablation in rabbits. We found that within 4 hours or the laser procedure, the nuclei of degenerating keratocytes in the superficial

stroma had become highly reflective and condensed. While the cells generally retained their parallel orientations, uniformity had decreased. Mild edema contributed to the generalized haze in the otherwise empty background. At 31 hours, cell density was reduced. Surviving cells remained round to oval in shape. By then, much of the edema had cleared, coincident with full re-epithelialization. At 4 days, the distinction between the fibrous and cellular elements had become increasingly blurred.

Increasing the depth of laser ablation was associated with a more protracted initial phase of keratocyte degeneration and a delay in the onset of scar formation. This contrasts with the degenerative changes in corneas with shallow ablations.

After the epithelium healed, it was found to be thicker than it was in the pre-ablated state. The cell size was variable and slightly smaller than before treatment. Superficial cells were also more irregular in shape. Beneath the epithelium of the ablated area, the subepithelial stroma showed dense fibroplasia and scarring. The posterior stroma of the ablated corneas was essentially identical to untreated corneas. No abnormalities of the corneal endothelium were found, nor were there any detectable changes in Descemet's membrane.

In the second year of this study, we reported the results of a study in rabbits that were treated bilaterally with the excimer laser and assigned to three treatment groups: pretreatment for one day with the PAF inhibitor LAU 0603, FML (fluorometholone, a mild ophthalmic steroid), or BSS (balanced salt solution, an inactive vehicle control). Treatment was started immediately after laser ablation and administered five times a day in an observer-masked study. Eyes were examined three times a week for eight weeks. We found that the 0.05% PAF inhibitor did not have any effect on the prevention

of corneal haze, but the use of the steroid FML prevented the appearance in a significant number of eyes. The animals with moderate to severe (grade 3 to 4) haze were then randomized to be treated with either the FML or BSS. The eyes were treated five times a day for seven additional weeks. We found that even the delayed use of the FML was effective in resolving the corneal haze.

2. Tear component contribution to damage

In the third year, our studies were directed to determining if the haze was being caused by something produced in the tears rather than as a direct result of the laser itself. We performed excimer laser ablation on rabbits, and immediately after treatment and before the eyelids could be blinked, one eye of each animal had a polymethyl methacrylate contact lens glues to the ablation area using tissue adhesive, in order to prevent the tears from reaching the wounded area. The other eye served as a control. Lenses were removed from the corneas at varying times, from one day to six weeks. We found that when the contact lens was allowed to remain on the cornea for only one day, both corneas developed minimal but similar haze.

We believed that the tears are involved in the process of producing the haze seen after even very superficial and short-term laser beam impingement on the cornea. To this end, we have been assessing methods for analyzing the tears from individual humans or animals without the necessity of pooling tears in order to obtain sufficient quantities for analyses, including capillary electrophoresis and matrix-assisted laser desorption/ionization mass spectrometry (MALDI). Analyzing tear samples smaller that 1 μl, we have found differences in the tears of individuals before and after laser treatment of the cornea. Some of the peaks are unique to pre-laser tears and others

are unique to post-laser treatment tears. Identification of the peaks is still in process.

3. Substance P in tears

This year, we have been studying other substances identified in the tears, especially P in human tears measured by laser desorption mass spectrometry and immunoassay. Substance P is a neuropeptide that promotes secretion by exocrine glands (1) and may act as a neurotransmitter or modulator in the central and peripheral nervous system (2). A substance P-like material is present in homogenates of the choroid, retina, optic nerve, optic nerve head, uvea, iris sphincter region, iris dilator and ciliary body, conjunctiva, whole upper eyelid, lacrimal gland, Harderian gland, and extraorbital muscle of the rabbit eye (3,4,5). In the densely innervated cornea (6), sensory fibers are positive for substance P (3). Substance P normally is not present or is present only in very low amounts in the aqueous humor of rabbits (5), but a peptide with substance P-like immunoreactivity is released into the aqueous humor when the trigeminal nerve is stimulated (7).

In lacrimal gland sections from rats, guinea pigs, and monkeys, nerve fibers that are immuno-histochemically positive for substance P or substance P-like material are located around blood vessels and ducts (8, 9). Based on these findings, Nikkinen et al. (9) and Matsumoto et al. (8) suggested that substance P may be an important modulator of lacrimal gland secretion. In support of this, Williams et al. (10) demonstrated that the number of nerves staining positively for substance P or substance P-like material in rat lacrimal glands declines as the animal ages, and suggested that the decline in substance P-containing nerves corresponds with and may be a contributing factor to reduced tear output in older animals. Another possible role

of substance P may be in promoting cellular growth (11, 12) and the production of extracellular matrix (11).

Substance P has recently been detected in human nasal lavage fluid (13). Because lacrimal secretions contribute to nasal fluids via the tear drainage system, it is reasonable to suspect that substance P also occurs in tears.

Methods. In this study, we used matrix-assisted desorption/ionization mass spectrometry (MALDI) and the enzyme-linked immunoabsorbant assay (ELISA) to determine whether substance P can be detected in human tears. MALDI was employed because it is sensitive to the low femtomole range, requires less than a microliter of sample, and is tolerant of salts and other impurities in the complex mixtures typical of body fluids (14). ELISA was used to confirm the MALDI results.

Unstimulated tears (approximately 10 μl/min) were collected from the inferior cul-de-sac with fire-polished 10 μl micropipettes. After collection, tears were either used immediately or stored in capped, 400 μl polyethylene micro centrifuge tubes at -20°C. Tears were collected from one eye of each of 12 healthy subjects. Subjects age ranged from 26 to 60 years. Six subjects were men and six were women. Eight subjects had normal eyes, i.e. were disease-free and did not wear contact lenses; four subjects had been diagnosed with dry eye syndrome. Dry eyes were associated with wearing contact lenses for two subjects, with rheumatoid arthritis for one subject, and with an unknown etiology to another subject, although the latter subject had mild anterior blepharitis, possible insufficient night-time lid closure, and a familial history of arthritis and lupus. Five of the eight subjects with normal eyes were excimer laser photo refractive keratectomy (PRK) patients, and their tears were collected before

surgery and on the first and/or second day after PRK. Seven postoperative samples were collected, but one preoperative sample was lost. Thus, a total of 18 tear samples were analyzed.

For MALDI, each tear sample was mixed 1:100, v:v, with matrix. The matrix was freshly prepared daily by dissolving an excess of α-cyano-4-hydroxycinnamic acid (Aldrich Chemical Co., Milwaukee, WI) in HPLC-grade acetonitrile containing 0.1% trifluoroacetic acid and diluting the result solution 1:1, v:v, with an aqueous solution of 0.1% trifluoroacetic acid. A 0.5 μl aliquot of tear-matrix solution was spotted on a stainless steel plate and allowed to air-dry for a few min until crystals of matrix and embedded protein formed (15). The plate was then introduced into a linear MALDI time-of-flight mass spectrometer (Voyager™ Biospectrometry™ Workstation, PerSeptive Biosystems, Framingham, MA) for analysis. The final mass spectrum generated from the analysis of each sample was averaged over 256 individual single-pulse spectra.

To prepare the standard solutions, substance P was obtained commercially (Cat # S 6883, Sigma Chemical Co. St. Louis, MO) and reconstituted in physiologically balanced, unpreserved sterile salt solution (Alcon Laboratories, Inc., Fort Worth, TX) at concentrations ranging from 10^{-4} to 10^{-12}M (1.35 picograms/ml). Balanced salt solution containing sodium, potassium, calcium, and magnesium salts was used, because it is similar to the aqueous phase of tears. Aliquots of the standard substance P solutions were mixed with the α-cyano-4-hydroxycinnamic acid matrix and processed for mass spectrometry in the same manner as the tear samples.

Results. To construct the mass spectra for the tear samples and substance P

standards, the ratio of mass to charge (m/z) was plotted on the abscissa and signal intensity in arbitrary units was plotted on the ordinate (Figs. 1 and 2). Figure 1 is a spectrum of a human tear sample. In Figure 2 (top), a part of the spectrum from Figure 1 was enlarged to show substance P at m/z = 1351 and oxidized substance P at m/z = 1366; for comparison , spectra of a subsample of the tears from Figure 1 with substance P added (Fig. 2, middle) and a substance P standard(Fig. 2, bottom) were included. All of the 18 tear samples analyzed with MALDI showed a well-defined peak in the m/z range from 1343.7 to 1355.9 or from 1356.9 to 1364.7. These results corresponded to an average m/z of 1349.8 $\pm$ 1.13 for protonated substance P $[M + H]^+$ and 1361.2 $\pm$ 0.54 for oxidized substance P $[M + O + H]^+$ obtained from the 14 mass spectra of substance P standards with concentrations ranging from 10^{-4} M to 10^{-12} M.

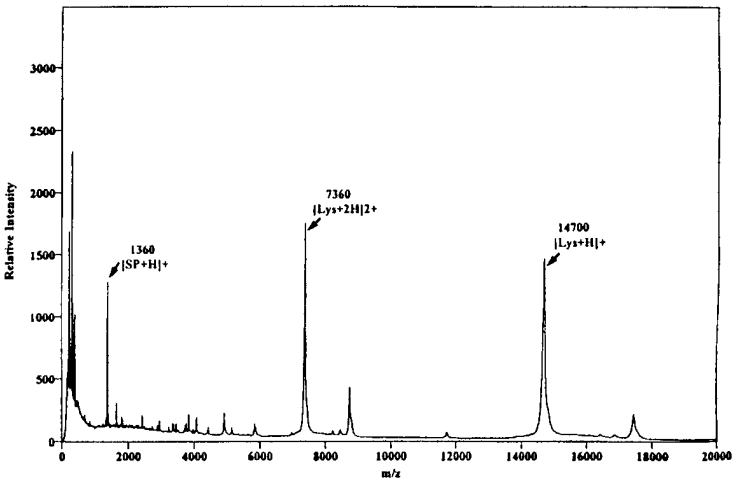

Figure 1. A MALDI mass spectrum of substance P (m/z = 1360) naturally occurring in undiluted tears collected from a healthy 28-year-old man who did not wear contact lenses and who was asymptomatic for dry eye syndrome. Lys+H and Lys+2H are lysozyme and its doubly protonated form, respectively (2).

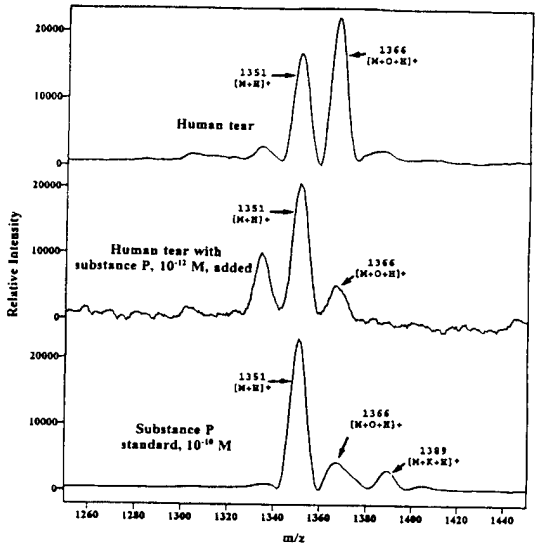

Figure 2. Top: The mass spectrum of substance P (m/z = 1351) in human tears from Figure 1. Middle: Tears from the same subject with substance P added at a concentration of 10-12 M. Bottom: Substance P standard at a concentration of 10^{-10} M in saline solution. In each tracing, the peak at m/z = 1366 is oxidized substance P. In the bottom tracing, the peak at m/z = 1389 is the potassium adduct of substance P; the potassium is provided by the saline solution.

A few other peaks in Figures 1 and 2 were tentatively identified. In Figure 1, peaks with m/z = 14,700 and m/z = 7360 appeared to be the singly protonated and doubly protonated ions of lysozyme, because they coincided with these peaks in the mass spectrum of the enzyme, as previously reported (16). In the mass spectrum of the substance P standard (Fig. 2, bottom), the low intensity peak at m/z = 1389 probably was the potassium adduct of substance P, which was contributed by the balanced salt solution. The difference in the m/z between the peak for substance P and the peak for the adduct was 38 mass units, which was within experimental error for the measurement of potassium at 39 mass units. When the standard solution was added to tears (Fig. 2, middle), the potassium-adduct peak was absent from the spectrums and presumably was suppressed. Other peaks in Figure 1 and 2 were identified.

An Enzyme Immunoassay Kit (Cat # 583751, Cayman Chemical, Ann Arbor, MI)

for substance P was used for ELISA analysis of tears. Tears from one eye of one subject (a woman) were collected and frozen at -20°C until 100 μl had been obtained, then pooled and divided equally into two wells of the test plate, in accordance with manufacturer's directions. The analysis was performed in duplicate. Substance P was detected in both replicates. The concentration of substance P in the tears from this subject was 125 pg/ml (9.26×10^{-11}M).

These findings demonstrate that substance P is a component of the tears obtained from normal eyes of men and women ranging in age from 26 to 60 years, from eyes fitted with contact lenses, from eyes with dry eye syndrome, and from eyes 1 to 2 days after excimer laser refractive surgery. However, we have not yet determined whether the concentration of substance P in tears varies with sex age, or eye conditions, and the source of substance P and its role in tears remain to be discovered.

REFERENCES

1. Rudich L, Butcher FR: Effects of substance P and eledoisin or K efflux, amylase release and cyclic nucleotide levels in slices of rat parotid gland. Biochim Biophys Acta 444:704-711, 1976.
2. Hokfelt T, Johansson O, Ljungdah A, Lundberg JM, Schultzberg M: Peptidergic neurones. Nature 284:515-521, 1980.
3. Butler JM, Powell D, Unger WG: Substance P levels in normal and sensorially denervated rabbit eyes. Exp Eye Res 30:311-313, 1980.
4. Butler JM, Ruskell GL, Cole DF, Unger WG, Zhang SQ, Blank MA, McGregor GP, and Bloom SR: Effect of VIIth (facial) nerve degeneration on vasoactive intestinal polypeptide and substance P levels in ocular and orbital tissues of the

rabbit. Exp Eye Res 39:523-532, 1984.

5. Unger WG, Butler JM, Cole DF, Bloom SR, McGregor GP: Substance P, vasoactive intestinal polypeptide (VIP) and somatostatin levels in ocular tissue of normal and sensorially denervated rabbit eyes. (Letter). Exp. Eye Res 32, 797-801, 1981.

6. Rozsa A, Beuerman RW: Density and organization of free nerve endings of rabbit corneal epithelium. Pain 14:105-120, 1982.

7. Bill A, Stjernschantz J, Mandahl A, Brodin E, Nilsson G: Substance P: release on trigeminal nerve stimulation, effects in the eye. Acta Physiol Scand 106:371-373, 1979.

8. Matsumoto Y, Tanabe T, Ueda S, Kawata M: Immunohistochemical and enzyme histochemical studies of peptidergic, aminergic and cholinergic innervation of the lacrimal gland of the monkey (Macaca fuscata) J Uton Nerv Syst 37:207-214, 1992.

9. Nikkinen A, Lehtosalo JL, Uusitalo H, Palkama A, Panula P: The lacrimal glands of the rat and the guinea pig are innervated by nerve fibers containing immunoreactivities for substance P and vasoactive intestinal polypeptide. Histochemistry 81:23-27, 1984.

10. Williams RM, Singh J, Sharkey KA: Innervation and mast cells of the rat exorbital lacrimal gland: the effects of age. J Auton Nerv Syst 47:95-108, 1994.

11. Reid TW, Murphy CJ, Iwahashi C, Fontes BA, Mannis MJ: Stimulation of epithelial cell growth by the neuropeptide substance P. J Cell Biochem 52:476-485, 1993.

12. Reid T, Nilsson J, von Euler AM, Dalsgaard CJ: Stimulation of connective tissue cell growth by substance P and substance K. Nature 315:61-63, 1985.

13. Schultz KD, Furkert J, O'Conner A, Bottcher M, Schmidt M, Baumgaretn CR, Kunkel G: Determination of substance P in human nasal lavage fluid. Neuropeptides 30: 117-124.

14. Hillenkamp F, Karas M, Beavis RC, Chait BT: Matrix-assisted laser desorption/ionization mass spectrometry of biopolymers. Anal Chem 63:1193A-1203A.

15. Beavis RC, Chaudhary T, Chait BT: α-Cyano-4-hydroxycinnamic acid as a matrix for matrix-assisted laser desorption mass spectrometry (Letter). Organic Mass Spectrom 27:156-158, 1992.

16. Maitchouk DY, Varnell RJ, Beuerman RW, Yan J: Analyzing proteins in tears from patients with dry eye syndrome, with contact lenses, or undergoing photorefractive keratectomy (PRK). (Abstract). Invest Ophthalmol Vis Sci 37, S18.

B. Evaluate drugs to prevent retinal damage after laser injury

It was not possible, as of the date of this report, to construct an adequate retinal objective for the confocal microscope. Three objectives were designed and constructed by optical engineers, however, each lens proved to be inadequate. Patient movement, decreased depth of field, varying dioptric corrections of the eyes, and varying lengths of the globes, proved to be a challenge in the design of these lenses. Further attempts at designing a retinal objective will continue in the future.

C. Study traumatic and non-traumatic glaucoma to determine its pathogenesis

Glaucoma is a disease that involves two separate pathologic processes. In those forms of the disease in which intraocular pressure is elevated, damage to the trabecular meshwork of the eye has occurred. For active duty military, the most important etiologies for this damage are related to ocular trauma and its primary and secondary effects on the trabecular meshwork. Within the retired military population, the separate etiologies contributing to trabecular meshwork damage in chronic open angle glaucoma (the most common form of glaucoma, particularly in the elderly) are most important.

We spent the first year establishing the laboratory and acquiring the necessary equipment to evaluate optic disc compliance as a measure of the mechanical behavior of the structural tissues of the optic disc. Initial mechanical testing sessions using the LDT scanning laser ophthalmoscope suggest that variability may be sufficient to allow pixel by pixel mapping of the optic disc surface changes.

In the second year, we reported that seven monkeys were imaged following the onset of glaucoma, and several more were into the lasering phase. Over 5000 images were obtained and saved in their entirety to optical discs. Image alignment and data processing has progressed through preliminary forms. Studies were also begun to determine the overall tilt that occurs in the posterior pole of the eye following acute pressure elevations, as well as the regional behavior of the surface of the optic nerve head and peri-papillary retina.

In the third year, we reported that we were analyzing preliminary results from two large experiments in which the confocal scanning laser ophthalmoscope was used to

study the onset of glaucomatous damage to the tissues of the optic nerve head.

During the last year of the study, we have been analyzing the preliminary results from two large experiments in which the confocal scanning laser ophthalmoscope has been used to study the onset of glaucomatous damage to the tissues of the optic nerve head. The following is an account of our progress.

1) Study 01 (our laboratory numbering system)**: Previously entitled: Characterization of early, middle, and late changes in the surface of the optic nerve head in experimental glaucoma by confocal scanning laser ophthalmoscopy; now referred to as the LSU Experimental Glaucoma Study (LEGS) .** The first study our laboratory has embarked upon is the characterization of the progressive changes in the optic nerve head surface that occur throughout the course of typical "glaucomatous" damage. Our goal in this study is to develop an extensive library of confocal scanning laser ophthalmoscopic images in which normal variation as well as early, middle and late glaucomatous changes are well catalogued. These images will then become the data base from which statistical strategies for the detection of optic nerve head change will be constructed. Finally, once we have decided on the proper way to detect change, these images will allow us to definitively describe the observed phenomena. That is, we hope to provide the first extensive description of the pattern of optic nerve head surface change that occurs in glaucomatous damage using images acquired with a confocal scanning laser ophthalmoscope (CSLO).

Table 1. Schedule of LEGS Imaging Sessions

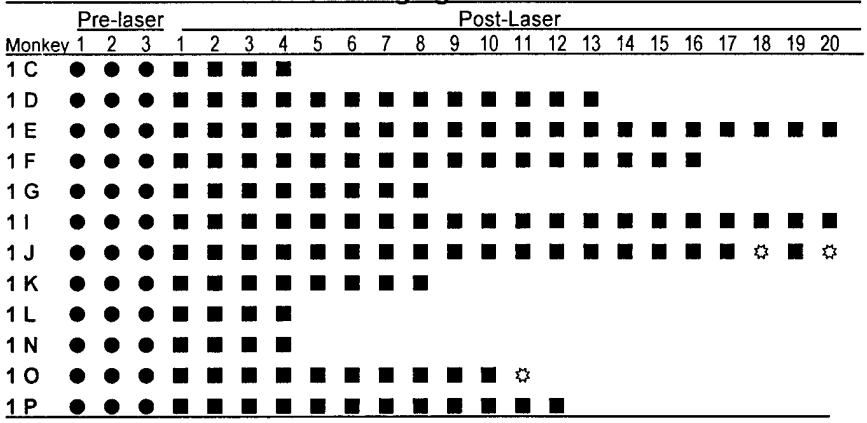

In the LEG study (Table 1), both normal eyes of 12 monkeys were imaged in three individual imaging sessions (performed on three separate days), separated by at least 2 weeks (the *pre-laser* imaging sessions). The trabecular meshwork of one eye (study eye) of each monkey was then treated with Argon Laser to induce elevated IOP. The ONHs of both eyes of each monkey (the study eye and the normal contralateral eye) were then imaged every 2 weeks (the *post-laser* imaging sessions) through the onset and progression of glaucomatous damage in each monkey's study

Table 2. LEGS Imaging Session Observation Points

	Observation	# Images	Observation Point Experimental Conditions		
Eye	Point	Acquired	IOP	10/15 degree image	EKG-linked
Study Eye	**01**	6	Physiologic	10 degree	EKG
	02	6	Physiologic	15 degree	EKG
	03*	6	IOP 10, 60 min	10 degree	non-EKG
	04*	6	IOP 10, 60 min	15 degree	non-EKG
	05	6	IOP 10, 90 min	10 degree	EKG
	06	6	IOP 10, 90 min	15 degree	EKG
	07	4	ONH stereo photographs		
Contralateral	**11***	6	Physiologic	10 degree	non-EKG
Normal Eye	**12***	6	Physiologic	15 degree	non-EKG
	13	4	ONH stereo photographs		

* Subset of images to be used in Phase 1

At each LEGS imaging session, six CSLO images of the ONH were acquired at each of a series of eight CSLO-observation points and four standard stereoscopic photographs were acquired at each of two additional stereo photographic-observation points (Table 2). Each imaging session observation point of the LEG study thus represents a longitudinal library of images obtained within one set of experimental conditions. The LEGS library is actually a series of libraries which can each be processed separately and then compared. Overall, the LEGS libraries were designed to include 1) images that characterize the variability inherent to imaging an unchanging eye over time (images of each study eye at each of its three *pre-laser* imaging sessions and images of each contralateral normal eye at a variable number (7 to 23) of *pre-* and *post-laser* imaging sessions) and 2) images that characterize the onset and progression of true glaucomatous ONH surface change (images of each study eye at each of its *post-laser* imaging sessions).

Strategies for image alignment and data processing have progressed through many preliminary forms. Figure 1 demonstrates the location of reference regions within an CSLO image, the LSU regional analysis strategy and our global summary parameter Mean Position of the Disc (MPD). An example of the Minimum Detectable Change for a series of LSU regional parameters and MPD is demonstrated in Table 3. The magnitude and location of the onset of statistically significant glaucomatous damage are demonstrated for the same parameters in Table 4.

During the past year, all images from observation points 03, 04,11 and 12 (Table 2) for all imaging sessions for all monkeys (Table 1 - a total of 4056 digital images) have been registered using the LDT software and the data has been exported to our SAS statistical programs within our laboratory computer. We are now in the process of constructing statistical strategies within the SAS software for the statistical determination of optic nerve surface change.

3) Study 04 (our laboratory numbering system)**: Regional Compliance of the Normal and Glaucomatous Monkey Optic Disc.** The second major study we have begun is a direct follow up to the work on compliance testing we have previously published. Our principal goals are to define the overall tilt that occurs in the posterior pole of the eye following acute pressure elevations, as well as the regional behavior of the surface of the optic nerve head and peripapillary retina.

This study, as well as study 01 above, utilizes the system for rapid confocal scanning laser image acquisition and data analysis that was described in our previous progress report and is now fully operational in our laboratory. Our system allows us to

acquire 6 to 10 images of the optic nerve head at a given observation point (any point in time at which we wish to characterize the position and/or configuration of the surface of the nerve head). Each image is then "registered" or "aligned" to a reference image for that eye and the elevation value for each pixel location is transferred to our Silicon Graphics INDY, where data are automatically entered into SAS statistical software, and mean data for each pixel value are generated for the 6 to 10 images. At present, the data for the 6 images we routinely require at an observation point are processed and available to us in 10 minutes as an "Observation Point summary form" (example in addendum). In addition we have now built the ability to look at the results of one complete compliance testing session with the position of the ONH tissues at each observation point (relative to position at the **BASELINE** observation point) color mapped (Figure 2).

This study has implemented a group of protocols in which the optic nerve head was imaged at a series of observation points at low and high intraocular pressure. The study is now completed and consists of a total of 83 compliance tests, performed on 16 eyes of 12 monkeys. All images from each compliance testing session have now been registered (approximately 4000 images) and the data again exported to our SAS statistical programs. We are in the middle of an extensive statistical analysis of the data from which we hope to construct simple, parameters that are sensitive to small, IOP-induced changes in the ONH.

1. **In vivo confocal microscopy of the movement of micro beads through aqueous outflow pathway for the study of glaucoma and its pathogenesis.**

   Glaucoma is a heretogeneous group of heterogeneous group of diseases, all of

which lead to optic nerve damage and visual loss usually as a result of increased pressure in the eye caused by impaired fluid outflow.1 The most prevalent type, primary open-angle glaucoma, is a leading cause of blindness throughout the world.[1-4] The prevalence of open-angle glaucoma was reported to be 6.3% in a group of elderly persons in California.[4] Another study showed that the prevalence varies from country to country in northern Europe.[3] Although the cause of this blinding eye disease remains unknown, the population at risk is growing, particularly with the aging of the "baby boomer" generation in the United States. It has been estimated that nearly 2.5 million persons in the U.S. will be afflicted with this disorder by the turn of the century.[5]

In open-angle glaucoma, restriction of the outflow of aqueous humor from the interior of the eye to the venous drainage system is thought to involve impeded passage through a narrow cleft of loose fibrous tissue, the trabecular meshwork. Recently, a gene has been discovered that encodes a trabecular meshwork protein, and a mutation of this gene appears to be associated with patients who have primary open-angle glaucoma.[6] Possible causes of failure of outflow, and hence the damaging rise in intraocular pressure, include pathologic changes in the structure of the meshwork and/or obstruction of the aqueous pathway by collapse of the channels carrying fluid away from the meshwork.[7-9] It has also been suggested that not all cases of glaucoma are caused by the same mechanism. Diagnosis and determination of the prognosis for a given patient require intraocular pressure measurements, visual fields testing, and evaluation of the anterior chamber angle. Studies in rabbits and monkeys involving experimental manipulation of intraocular pressure are inconclusive in their elucidation of the outflow mechanisms.[10, 11] To date, direct evaluation of the structures

of the aqueous outflow pathway at the cellular level has not been possible; with the new confocal microscopy methodology described in this study, such an approach may become practical and useful in both diagnosis and the determination of optimal therapy.

The white-light confocal microscope provides in vivo cellular level analysis of events such as fibroblast activation and epithelial wound healing. Confocal microscopic measurement and morphological characterization of cells in the living eye allow precise identification of phenotype for both tissue cells and cells of immune origin.[7-9,12-14] White-light confocal microscopy is non-destructive, permitting repeated in vivo observations of cellular processes, such as migration of inflammatory cells from the vascular space, fibroblastic activation of cells, and the response to chemical manipulation and disease processes, over time. [15,16]

The outflow pathway in the rabbit has structural components analogous to those of the primate; fluid drains from the anterior chamber into a fibrous meshwork, thence into the aqueous plexus, and finally into venous collecting channels. The aqueous plexus -- Fontana' s space in rabbits, Schlemm's canal in primate -- has been difficult to separate from the trabecular meshwork as a cause of increased intraocular pressure, because it has not been possible to directly observe changes in its dimensions or the through-flow into the aqueous drainage system in the living eye. In this study, we demonstrate that, with confocal microscopy, it is possible to observe micro beads injected into the anterior chamber of normal rabbit eyes moving in the anterior chamber and in the aqueous plexus. By measuring the differential velocity of flow in these structures, the presence of an intervening resistance, probably the fibrous trabecular meshwork, may be inferred.

METHODS

Animal care and treatment in this investigation were in compliance with the ARVO Resolution on the Use of Animals in Research. New Zealand white rabbits (2-3 kg) were anesthetized by intramuscular injection of ketamine hydrochloride (30 mg/kg) and xylazine (6 mg/kg). A 6-0 suture to adjust eye position was attached to a superficial location approximately at the 12:00 o'clock position. The rabbits were wrapped in a pad to maintain body temperature and positioned on their side in a specially designed holder. The eyelids were held open by a wire speculum.

An aliquot of 7.4 x 10^5 micro beads/ml in water was diluted with sterile 0.9% NaCl, such that a 5-μl aliquot contained 3.7 x 10^4 micro beads. For each observation, a 5 μl aliquot was injected into the anterior chamber of the rabbit eye over a period of 5 minutes (Fig. 1). The micro beads (Bangs Laboratories, Inc., Fishers, Indiana) were made of polystyrene without surface functional groups and contained a black organic nonpermeable material. The micro beads were 2.5 μm $\pm$ 10% in diameter, with a density of 1.05 g/ml.

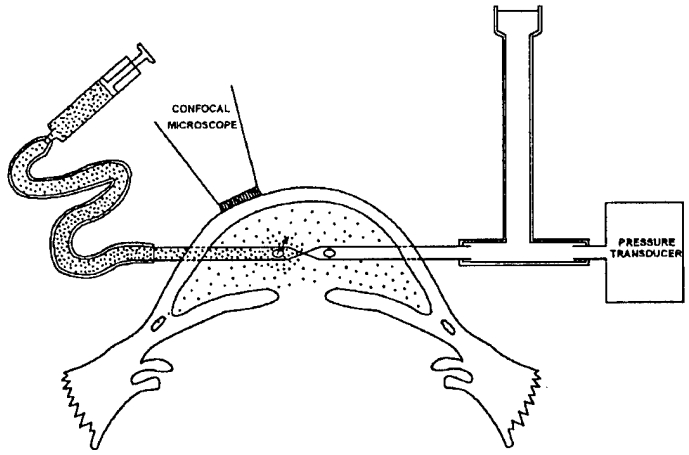

Fig.1. Schematic diagram of ocular preparation for confocal microscopy of micro bead movement through the anterior chamber and aqueous plexus. A needle inserted across a corneal diameter allowed measurement of the intraocular pressure during injection of 5-μl aloquot of a sodium chloride solution containing the micro beads. Intraocular pressure was held constant by the saline column. The objective of the confocal microscope was moved around to visualize the aqueous outflow pathway. The layer of methyl cellulose used as an optical coupler is indicated by the lined segment between the objective of the confocal microscope and the corneal surface; the thickness of the layer is exaggerated for visibility.

For confocal microscopy, as in previous studies on humans and animals,[14,16] the cornea was covered with an optically thin layer of 10% methyl cellulose and the convex surface of the objective was brought into position. Images were viewed as the plane of focus was moved through the tissue in increments of a few microns, with the confocal microscopic images viewed in real-time on a video monitor (Sony Medical Monitor) and recorded through a CCD camera (Videoscope, Washington, DC) onto S-VHS tape for later playback and analysis.[14, 16]

To determine the average velocity of the micro beads in the anterior chamber and Fontana's space, individual frames were captured from S-VHS videotape every 0.2 seconds on an Epic 2MEG (Epic, Buffalo Grove, Illinois) frame grabber and transferred to Optimas software (Optimas Corp., Seattle, Washington). Pixel to micrometer conversion was made for the images. Instantaneous velocity for each time point was calculated by determining the change in position for each time point; mean velocity was calculated as the average of all of the instantaneous velocity calculation for each time and position.

At the conclusion of the experiment, the animals were killed by an overdose of sodium pentobarbital. The eye was initially fixed by immersion in a fixation solution, frozen, and prepared for cryostat sections (7 μm). Dark field microscopy and photography were performed using a Leica research microscope.

RESULTS

Rabbits were anesthetized and 9-0 sutures (30 μm diameter) were placed at the corneoscleral limbus (the junction between the cornea and the sclera) to identify the area during confocal microscopy. A 23-gauge needle with a constriction half way along

its length and having small holes above and below the constriction was introduced transcorneally, avoiding contact with the iris (Fig. 1). One end of the needle was connected by polyethylene tubing to a 10-μl syringe and the other end to a reservoir containing Ringer's solution and a pressure transducer to prevent changes in intraocular pressure. Micro beads were injected into the anterior chamber slowly over 5 minutes. The objective of the confocal microscope was carefully brought into position. A thin layer of 10% methyl cellulose was used as an optical coupler; there was not direct contact between the eye and microscope. The three layers of the cornea (epithelium, stroma, and endothelium) were identified.[7-9, 12,13]

As the objective of the confocal microscope was moved across the corneal surface toward the periphery where the cornea meets the sclera, micro beads were observed in the aqueous humor just posterior to the endothelium (Fig. 2) and at the anterior surface of the iris (not depicted). The vessels of the conjunctiva and the flow of red blood cells and cells of immune origin were noted as the plane of focus moved downward at the corneoscleral limbus. Micro beads in the anterior chamber were recorded on video tape for up to 20 seconds. The mean velocity of the micro beads in the anterior chamber was determined to be 7.2 μm/sec $\pm$ 0.38 μm/sec (n=5).

Micro beads that had been injected into the anterior chamber were observed in vivo by confocal microscopy in the aqueous plexus (Fontana's space) (Fig. 3). The mean velocity of the micro beads in Fontana's space was found to be 64.3 μm/sec $\pm$ 3.1 μm/sec (n=5) (Fig. 3), which was significantly faster than the rate in the anterior chamber ($p > 0.01$). Confocal microscopy showed the opaque suture, which was approximately 30 μm in diameter, above Fontana's space; the diameter of Fontana's

space varied from 30 to 50 μm. A venous collecting channel was seen to open directly into this space (Fig. 3). Histological analysis (Fig. 4) also identified the connection between the aqueous plexus and the venous collecting channels seen in vivo by confocal microscopy (Fig. 3). An accumulation of micro beads in Fontana's space was identified in frozen sections, and the variable diameter of this space previously measured by confocal microscopy was verified (Fig. 4). The appearance of these structures as seen by confocal microscopy, as well as our histological results, are corroborated by an earlier histological study of the rabbit outflow pathway.[17]

DISCUSSION

The clinical ability to visualize the outflow apparatus in the glaucomatous eye in humans may lead to increased understanding of the disease, the ability to diagnose the early signs of the disease, and based on the site of the outflow abnormality, the individualization of therapy to the specific type of glaucomatous pathology. Glaucoma is treated by several modalities, including drugs, laser surgery, and filtration surgery; the ability to visualize the outflow pathway provides a direct means of observing the therapeutic effects. Some of the mechanisms that cause various types of glaucoma, such as the elevated intraocular pressure induced by the therapeutic use of corticosteroids, may be different from the mechanism that causes primary open-angle glaucoma. Modification of this technique to improve our understanding of the dynamics of aqueous humor outflow in humans may lead to improved therapeutic measures. The ability to correlate structural changes in the trabecular meshwork and Schlemm's canal in the living human eye with the type of glaucoma could provide new insights into this blinding eye disease.

Additionally, this new application of confocal microscopy, in conjunction with the appropriate tracers (or stains), will give us a unique new experimental tool to evaluate the flow of aqueous humor in glaucoma. For the first time, we can directly evaluate the rate of movement of aqueous humor through the anterior chamber angle. This also provides a potentially powerful tool to evaluate the effect of new glaucoma drugs with respect to their ability to change the structural resistance (flow) of the components that make up the outflow pathway. In particular, confocal microscopy may be useful to better understand the contribution of uveoscleral outflow to the intraocular pressure regulation, which is not well understood.[18, 19]

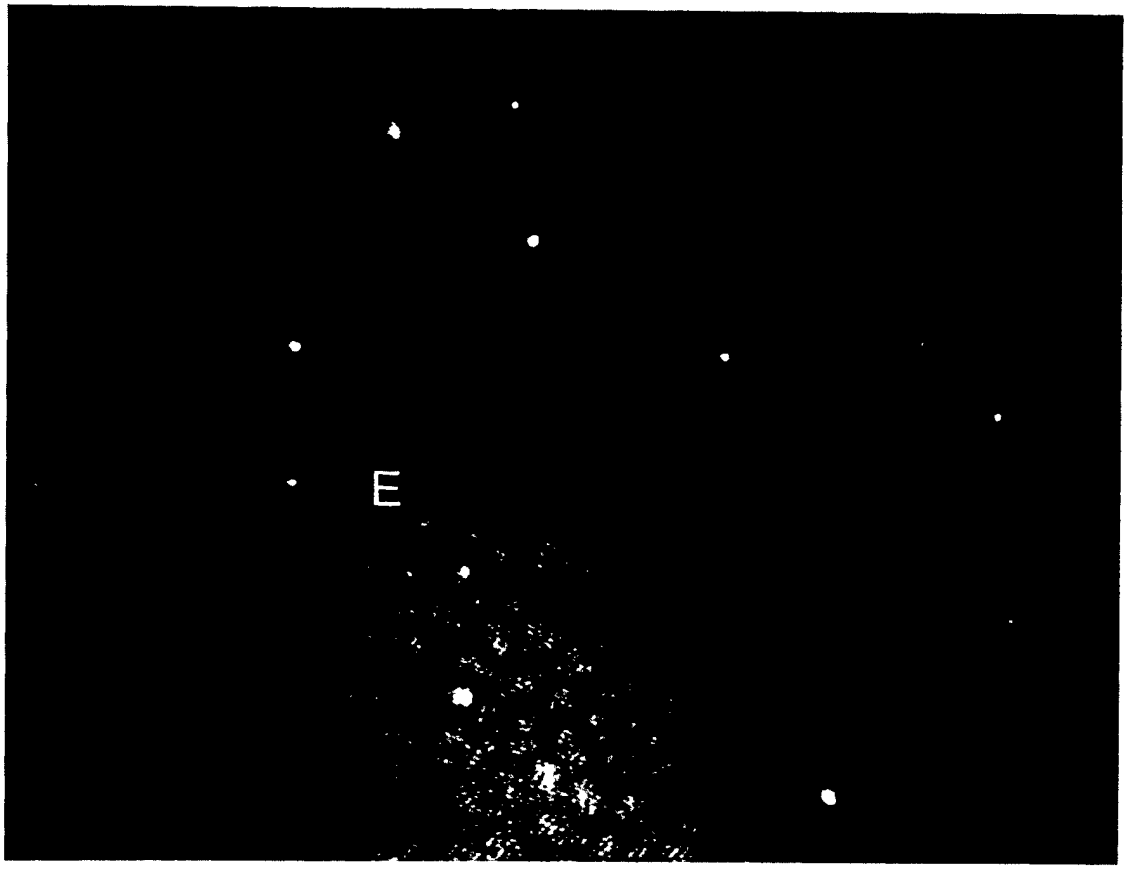

Figure 2

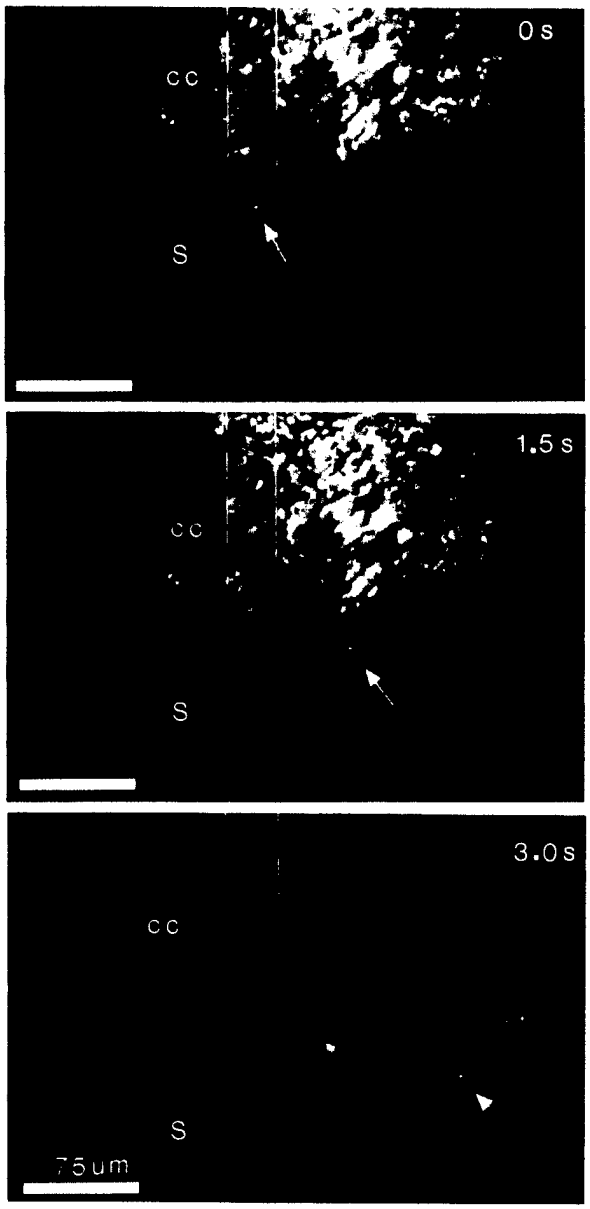

Figure 3

Figure 4

FIGURE LEGENDS

Fig. 2. Confocal micrograph of micro beads in the anterior chamber. The corneal endothelial cells (E) can be seen in outline. To view both the central and peripheral areas of the anterior chamber, the objective was moved over the corneal surface with adjustments for changes in corneal thickness. The outflow meshwork (not shown) was identified by its loose fibrous structure.

Fig. 3. Confocal micrographs of the movement of a single micro beadsin the fluid-filled space of Fontana. (A) This view shows bead movement beginning at an arbitrary time and location denoted by the parallel solid white lines. (B) The time is 1.5 sec after the view in (A), and the bead has moved 70.2 μm, giving a velocity of 83.8 μm/sec. © The bead has moved an additional 87.2 μm, giving a velocity of 81.2 μm/sec. A venous collecting channel (CC) and its opening into the space are visible in all three views. Compare the view in © with Figure 4. S, Fontana's space. Bar, 75 μm.

Fig. 4. Seven-micron-thick cryostat sections of the anterior chamber angle of the rabbit eye depicting the fluid and the flow structures. Top. Two collecting channels (CC) are seen to course outward from areas of the plexus close to Fontana's space (S). Note the ciliary processes (CP) at the bottom of the figure. The junction of the cornea (on the left) with the sclera (on the right), known as the corneoscleral limbus, is defined by the termination of Descemet's layer (D), which underlies only the cornea and does not extend beneath the sclera. AC, anterior chamber. (Magnification, x 130). Bottom.

In a higher magnification, the micro beads are visible just below Descemet's layer (D) and in Fontana's space (S), and the tubular nature of the collecting channels (CC) can be seen. D, Descemet's membrane (Magnification, x 328).

REFERENCES

1. Tielsch JM: The epidemiology and control of open angle glaucoma: a population-based perspective. Annu Rev Public Health 17: 121-136, 1996.
2. Nemesure B, Leske MC, He Q, Mendell N: analysis of reported family history of glaucoma: a preliminary investigation. The Barbados Eye Study Group. Ophthalmol Epidemiol 3:135-141, 1996.
3. Ringvold A: Epidemiology of glaucoma in northern Europe. Eur J Ophthalmol 6: 26-29, 1996.
4. Doughtery PJ, Englehardt RF, Lee DA: Eye disease among ambulatory Jewish senior citizens in California. J Community Health 19:271-284, 1994.
5. Quigley HA, Vitale S: Models of open-angle glaucoma prevalence and incidence in the United States. Invest Ophthalmol Vis Sci 38:83-91, 1997.
6. Stone EM et al.:Identification of a gene that causes primary open angle glaucoma. Science 275: 668-670, 1997.
7. Ten Hulzen RD, Johnson DH: Effect of fixation pressure on juxta canalicular tissue and Schlemm's canal. Invest Ophthalmol Vis Sci 37:114-124, 1996.
8. Allingham RR, de Kater AW, Ethier CR: Schlemm's canal and primary open angle glaucoma: correlation between Schlemm's canal dimensions and outflow facility. Exp Eye Res 62:101-109, 1996.
9. Grierson I, Nagasubramanian S, Edwards J, Miller LC, Ennis, K: The effects of various levels of intraocular pressure on the rabbit's outflow system. Exp Eye Res 42:383-397, 1986.
10. Tingey DP, Schroeder A, Epstein MP, Epstein DL: Effects of topical ethacrynic

acid adducts on intraocular pressure in rabbits and monkeys. Arch Ophthalmol 110: 699-702, 1992.

11. Finger PT, Moshfeghi DM, Smith PD, Perry HD: Microwave cyclodestruction for glaucoma in a rabbit model. Arch Ophthalmol 109: 1001-1004, 1991.

12. Chew SJ, Beuerman RW, Kaufman HE: Real-time confocal microscopy of keratocyte activity in wound healing after cyroablation in rabbit corneas. Scanning 16:269-274, 1994.

13. Chew SJ et al: Early diagnosis of infectious keratitis with in vivo real time confocal microscopy. CLAO J 18, 197-201, 1992.

14. Beuerman RW, Laird JA, Kaufman SC, Kaufman HE: Quantification of real-time confocal images of the human cornea. J Neurosci 54:197-203, 1994.

15. Cohen RA et al.: Confocal microscopy of corneal graft rejection. Cornea 14:467-472, 1995.

16. Kaufman SC, Laird JA, Cooper R, Beuerman RW: Diagnosis of bacterial contact lens-related keratitis with the white-light confocal microscope. CLAO J 22, 274-277, 1996.

17. Knepper PA, McLone DG, Goossens W, Vanden Hoek T, Higbee RG: Ultrastructural alterations in the aqueous outflow pathway of buphthalmic rabbits. Exp Eye Res 52: 525-533, 1991.

18. Poyer JF, Gabelt B, Kaufman PL: The effect of topical $PGF_{2\alpha}$ on uveoscleral outflow and outflow facility in the rabbit eye. Exp Eye Res 54: 277-283, 1992.

19. Camras CB, Bito LZ, Eakins KE: Reduction of intraocular pressure by prostaglandin applied topically to the eyes of conscious rabbits. Invest

Ophthalmol Vis Sci 16:1125-1134, 1977.

D. Study drugs that will prevent the recurrences of herpes

Recurrent herpes, both in the eye and elsewhere, is a major problem. There are some 500,000 cases of ocular herpes reported in the United States, and genital and labial herpes also represent a major clinical problem.

Systemic antiviral drug reduce the frequency of genital herpes while they are being administered, and prevent sores from developing, however, they do not prevent shedding of the virus and the infection of partners or the spread of disease. Systemic antivirals do not prevent recurrences of ocular herpetic disease. We believe that virus reactivates on the ganglion cells and travels to the periphery, where in the genitalia, shedding results; in the eye, even small amounts of virus produce corneal disease. The goal in both genital and ocular disease is to find a way to stop reactivation in the neural ganglia.

1. Thymidine kinase inhibitors. During the first year of our studies, we reported that we obtained a new thymidine kinase inhibitor, 9-(4-hydroxybutyl) -N^2-phenylguanine (or HBPG) from a collaborator at the University of Massachusetts Medical Center. Our first step was to determine the pharmacokinetics of this compound in the squirrel monkey. We found that the drug had a true elimination half-life of 12.5 hours when it was administered intra peritoneally, and determined that it was not stored in the fat.

In the second year, we tested HBPG in squirrel moneys to determine whether it was effective in reducing the clinical corneal recurrences of herpes virus. Based on our pharmacokinetic studies, we decided to treat the animals every eight hours with either HBPG suspended in corn oil or corn oil placebo. We pre-treated the animals with either drug or placebo, and then subjected than to a cold-stress for a short period of time to

induce ocular recurrences. We found that the frequency of recurrent herpetic keratitis in the HBPG-treated monkeys was lower than in the corn oil-treated monkeys. We also tested the HBPG in our mouse model of heat stress-induced reactivation, and found that the frequencies of infectious virus found in the tears and trigeminal ganglia were statistically significantly lower in HBPG-treated animals as compared to the placebo-treated animals, and the viral DNA expression in the trigeminal ganglia was also significantly lower. Attempts will be made by our consultant to produce a more soluble form of the HBPG because further studies are limited be the solubility of the drug.

2. Beta blockers. Also in the first year, we reported that we were studying beta blockers to reduce reactivation of virus from latency. The first compound that we tested was propranolol. In a mouse model or heat-stress reactivation of herpes, we determined that the animals treated with propranolol had a lower rate of shedding infectious virus in their tears than mice treated with placebo. We also determined that propranolol suppressed viral reactivation from the trigeminal ganglion s well as reduced the viral DNA in the trigeminal ganglia.

During the second year, we studied the effect of propranolol on spontaneous recurrences of ocular herpetic keratitis in the rabbit. Twenty one days after infection, rabbits were randomized to be treated either with propranolol twice a day or saline. We found that there was a significant difference in the ocular recurrences in the rabbits that were treated with the propranolol.

During the second year, we also tested another beta blocker, timolol maleate, in the mouse model. We found that pretreatment reduced the frequency that infectious virus was found in the tears and in the trigeminal ganglion.

During the third year, we treated the propranolol in our squirrel monkey model of recurrent herpetic keratitis. We were not able to show any effect of the propranolol, we believe, because of the very low recurrence rate of keratitis that we encountered. Using the mouse model of heat stress-related recurrences, we tested other beta adrenergic receptor blocking agents: penbutolol, betaxolol, metoprolol and ICI 118,551. Each of these agents, with the exception of penbutalol showed significant activity in inhibiting stress-induced viral reactivation.

At the end of the past grant year, we had just embarked on studies designed to determine if a variety of adrenergic receptor agonists could induce a viral reactivation and to determine if such a reactivation was related in a functional and physiological way, to our previous observations with beta adrenergic receptor agonists. In preliminary experiments, we had failed to find any activity of norepinephrine administered to mice at a concentration of 0.01 mg per animal per day. Additional studies with norepinephrine, isoproterenol, and ephedrine have yielded promising new results. These adrenergic receptor agonists when given to mice which are latent for HSV-1 were found to statistically significantly increase the frequency of viral shedding from the eyes of mice (Table 1). changes were made in the drug delivery system in that slightly higher concentrations of the receptor agonists were used and the duration of treatment was increased from 3 days to 5 days.

Further analysis of the results obtained using the adrenergic receptor agonists reveals that norepinephrine and isoproterenol are agonists which act on the beta adrenergic receptors whereas ephedrine is a receptor agonist of mixed activity for both alpha and beta adrenergic receptors. It is of interest that these compounds (Table 2)

which have activity for the beta receptors or for alpha beta receptors have a significant effect in stimulating a viral reactivation.

In a preliminary study completed just at the end of the current grant year, we investigated the relationship between corneal epithelial nerves and viral reactivation stimulated by adrenergic receptor agonists. Mice which were latent for HSV-1 were treated with a dilute solution of sodium hydroxide. This treatment causes the superficial most layer of epithelial cells to peel off and cauterizes the epithelial nerve endings. Latent mice treatment with sodium hydroxide and control mice were given injections of norepinephrine, and the frequency of viral shedding at the ocular surface determined. It was found within two weeks after hydroxide treatment the frequency of viral shedding was significantly reduced in the eyes of animals which had been treated with the dilute sodium hydroxide (Table 3). These preliminary results indicate that there is a direct connection between the effect of the adrenergic receptor agonists on receptor-expressing cells and the shedding of virus from the nerve endings in the corneal epithelium. Further studies on this observation are in progress.

Table 1
Viral Reactivation Following Adrenergic Receptor Agonists Treatment

Treatment	Infectious Virus (+ Eyes/Total Eyes)	Percent Positive
Norepinephrine	4/11	36
Isoproterenol	4/10	40
Ephedrine	4/12	33
Placebo	0/12	0
Stress	8/14	57

Latent mice were treated three times daily (0.02 mg/ml) for five days by intraperitoneal injection and tested for ocular shedding of virus on days 3, 5, and 7. The stressed mice were tested for virus 24 hours after thermal treatment.

Table 2
Receptor Agonist Specificity and Viral Reactivation

Agonist	Receptor Specificity		Effect on Reactivation (+ induces; - no effect)
	Mixed	Beta	
Norepinephrine		+	+
Isoproterenol		+	+
Ephedrine	+		+

Table 3
Requirement for Epithelial Nerve in the Agonist Induced Viral Shedding

Treatment	Infectious Virus (+ Eyes/Total Eyes)	Percent Positive
Dilute NaOH	3/20	15
Saline	10/22	45

Latent mice were topically treated with 0.001M NaOH or saline. Two weeks later they were given IP injections of norepinephrine as indicated in Table 1 above and viral shedding determined on days 3, 5, and 7.

E. Publications

1. Varnell RJ, Freeman JY, Maitchouk D, Beuerman RW, Gebhardt BM: Detection of substance P in human tears by laser desorption mass spectrometer and immunoassay. Curr Eye Res16:960-963, 1997.

2. Kaufman HE, Varnell ED, Thompson HW: Trifluridine, cidofovir, and penciclovir in the treatment of experimental herpetic keratitis. Arch Ophthalmol, submitted.

3. Palkama A, Beuerman RW, Ohta T, Kaufman SC, Laird JA, Kaufman HE: In vivo confocal microscopy of the movement of micro beads through the aqueous outflow pathway. Science, submitted.

4. Kaufman HE, Varnell ED, Wright GE, Xu H, Gebhardt BM, Thompson HW: Effect of 9-(4-hydroxybutyl)-N^2-phenylguanine (HBPG), a thymidine kinase inhibitor, on clinical recurrences of ocular herpetic keratitis in squirrel monkeys. Antiviral Res 3365-72, 1996.

5. Varnell RJ, Maitchouk DY Beuerman RW, Salvatore MF, Carlton JE: Analysis of rabbit tear fluid using capillary electrophoresis with UV of laser-induced fluorescence detection. J Cap Elec 004:1-6, 1997.

6. Beuerman RW: Editorial: Confocal microscopy: into the clinic. Cornea 14:1-2, 1995.

7. Chew SJ, Lam DSC, Beuerman RW, Kaufman SC, Kaufman HE: Evaluation of giant papillary conjunctivitis and allergic conjunctivitis with in vivo confocal microscopy. Ophthalmic Practice 13(1):11-14, 1995.

8. Kaufman SC, Beuerman RW, Greer DL: Confocal microscopy: a new tool for the study of the nail unit. A Am Acad Dermatol 32:668-670, 1995.

9. Gebhardt BM, Kaufman HE, Hill JM: Effect of acyclovir in thermal stress-induced herpesvirus reactivation. Antiviral Res, in press.

10. Cohen RA, Chew SJ, Gebhardt BM, Beuerman RW, Kaufman HE, Kaufman SC: confocal microscopy of corneal graft rejection. Cornea 14:467-472, 1995.

11. Chew SJ, Beuerman RW, Kaufman HE, McDonald MB: In vivo confocal microscopy of corneal wound healing following excimer laser photorefractive keratectomy. CLAO J 21:273-280, 1995.

12. Kaufman SC, Hamano H, Beuerman RW, Laird JA, Thompson HW: Transient corneal stromal and endothelial changes following soft contact lens wear: a study

with confocal microscopy. CLAO J 22:127-132, 1996.

13. Kaufman SC, Laird JA, Beuerman RW: In vivo immunofluorescent confocal microscopy of herpes simplex keratitis. SPIE, San Jose, CA, January, 1996. Proceedings of Ophthalmic Technologies VI, Volume 2673, pp. 2-5, 1996.

14. Laird JA, Beuerman RW, Kaufman SC: Quantification of confocal images of human corneal endothelium. SPIE, San Jose, CA, January, 1996. Proceedings of Ophthalmic Technologies VI, Volume 2673, pp. 224-227, 1996.

15. Kaufman SC, Beuerman RW, Goldberg D: A new form of primary localized corneal amyloidosis: a case report with confocal microscopy. Metabolic, Pediatric and Systemic Ophthalmology, in press.

16. Kaufman SC, Laird JA, Cooper R, Beuerman RW: Diagnosis of bacterial contact lens-related keratitis with the white-light confocal microscope. CLAO J, in press.

17. Gebhardt BM, Kaufman HE: Propranolol suppresses reactivation of herpesvirus. Antiviral Res 27:255-261, 1995.

18. Kaufman HE, Varnell ED, Gebhardt BM, Thompson HW, Hill, JM: Propranolol suppression of ocular HSV-1 recurrence and associated corneal lesions following spontaneous reactivation in the rabbit. Curr Eye Res 15:680-684, 1996.

19. Burgoyne CF, Varma R, Quigley HA: Clinical judgement compared with digitized image analysis in the detection of induced optic disc change. Am J Ophthalmol 120:176-183, 1995.

20. Burgoyne, CF, Varma R, Quigley HA at al: Global and regional detection of induced optic disc change by digitized image analysis. Arch Ophthalmol 112:261-268, 1994.

21. Chew SJ, Beuerman RW, Assoline M, Kaufman HE, Barron BA, Hill JM: Early diagnosis of infectious keratitis with in vivo real-time confocal microscopy. CLAO J 18:197-201, 1992.

22. Kaufman SC, Chew SJ, Capps SC, Beuerman RW: Confocal microscopy of corneal penetration of tarantula hairs. Scanning XXX.

ABSTRACTS:

XX. Hunt J, Qui L, Klyce N. Thompson HW, Burgoyne CF: Minimum detectable change (MDC) within regions of the optic disc and peripapillary retina in a longitudinal study of experimental glaucoma by confocal scanning laser

ophthalmoscopy (CSLO). ARVO abstract. Invest Ophthalmol Vis Sci Suppl 37:XXX, 1996.

Xx. Lam DSC, Chew SJ, Beuerman RW, Kaufman SC, Kaufman, HE: Low power telescopic confocal microscopy of the eye ARVO abstract ##2327. Invest Ophthalmol Vis Sci ABS 36:502, 1995.

Varnell RJ, Maitchouk DY, Rucker VC, Beuerman RW: The clinical potential of laser desorption mass spectrometry of tears. Pittsburgh Conference, 1997. Atlanta, GA.

Zhang DM, Beuerman RW, Zhao S, Tran H, Kline D, Gould H: Cellular factors involved in neuroma formation. Soc Neurosci ABS, Vol 21, Part 3, p. 1798, 1995.

Kaufman SC, Laird, JA, Beuerman RW: Human corneal endothelial cell quantification using white light confocal microscope images. Invest Ophthalmol Vis Sci ABS 37:83, 1996.

Burgoyne CF, Hunt J, Qiu L, Klyce N, Thompson HW: Change within regions of the optic disc precedes change within regions of the peripapillary retina in a longitudinal study of experimental glaucoma by confocal scanning laser ophthalmoscopy (CSLO). Invest Ophthalmol Vis Sci ABS 37 , 1996.

Thompson HW, Harlow CA, Beuerman RW, Burgoyne CF, Heickell AG: Discrete wavelet transforms as change detectors in optic disc images. Invest Ophthalmol Vis Sci ABS 37:, 1996.

Heickell AG, Thompson HW, Burgoyne CF: Regional compliance of the monkey optic disc and peripapillary retina by scanning laser ophthalmoscopy. Invest Ophthalmol Vis Sci ABS 37:, 1996.

Beuerman RW, Kaufman SC, Laird J, Kaufman HE: In vivo, real-time, immunofluorescence examination of corneal epithelium with the confocal microscope. Invest Ophthalmol Vis Sci ABS 36:698, 1995.

Chu, E, Chan TK, Chew SJ, Beuerman RW, Kaufman SC, Kaufman HE: In vivo confocal microscopy of the human eye in contact lens wear. Invest Ophthalmol Vis Sci ABS 36:1022, 1995.

Kaufman SC, Beuerman RW, Laird J: In vivo real-time confocal microscopy of fungal, bacterial, and acanthamoeba keratitis. Invest Ophthalmol Vis Sci ABS 36:1922, 1995.

Kaufman SC, Maitchouk DY, Yaylali V, Beuerman RW, Laird J: Confocal microscopic analysis of corneal neovascularization in rabbits. Invest Ophthalmol

Vis Sci ABS 38(4), 1997.

Yaylali V, Maitchouk DY, Kaufman SC, Beuerman RW, Laird J: Confocal microscopy of the rabbit conjunctiva and cornea and the response to wounding. Invest Ophthalmol Vis Sci ABS 38(4), 1997.

ELSEVIER

Antiviral Research 33 (1996) 65–72

Antiviral Research

Effect of 9-(4-hydroxybutyl)-N^2-phenylguanine (HBPG), a thymidine kinase inhibitor, on clinical recurrences of ocular herpetic keratitis in squirrel monkeys

Herbert E. Kaufman[a], Emily D. Varnell[a,*], George E. Wright[b], Hongyan Xu[b], Bryan M. Gebhardt[a], Hilary W. Thompson[a]

[a]*Lions Eye Research Laboratories, LSU Eye Center, Louisiana State University Medical Center School of Medicine, 2020 Gravier Street, Suite B, New Orleans, LA 70112, USA*

[b]*Department of Pharmacology, University of Massachusetts Medical School, Worcester, MA 01655 USA*

Received 27 March 1996; accepted 29 July 1996

Abstract

9-(4-Hydroxybutyl)-N^2-phenylguanine (HBPG) is a new viral thymidine kinase inhibitor that we tested for the ability to prevent recurrences of herpetic keratitis. Eighteen squirrel monkeys (*Saimiri scuireus*) were infected in both corneas with the Rodanus strain of herpes simplex virus type 1 (HSV-1). All corneas showed typical dendritic keratitis 3 days after infection, followed by spontaneous healing. On day 21, the monkeys were randomized into two coded groups and ocular examinations were begun. One group received intraperitoneal (i.p.) injections of HBPG, 150 mg/kg, in a corn oil suspension every 8 h, and the other group received i.p. injections of the corn oil vehicle only. On day 22, recurrences were induced by reducing the temperature of the room in the late afternoon so that a low of 18°C was achieved during the night. After the morning treatment, room temperature was raised to the normal ambient temperature (24–27°C), and treatment was discontinued. Treatment was reinstituted on day 27, the room temperature was lowered again on day 28, and treatment was again discontinued as before. Third and fourth cycles of treatment and cold stress were begun on days 34 and 69. Ocular examinations were continued until day 73, at which point the code was broken. We found that the HBPG treatment significantly reduced the number of corneas with recurrences during the treatment periods, compared with recurrences in untreated, cold-stressed animals ($P = 0.01$).

Keywords: Antiviral; Herpes simplex virus (HSV); Recurrent infections; *Saimiri scuireus*; Thymidine kinase

* Corresponding author. Tel.: + 1 504 5686700, ext. 336; fax: + 1 504 5684210; e-mail: evarne@lsumc.edu

PII S0166-3542(96)00997-7

1. Introduction

The herpes viruses are common pathogens in humans and a variety of animal species (Straus et al., 1985; Mertz, 1990). Herpes simplex virus type 1 (HSV-1) and herpes simplex virus type 2 (HSV-2) infect epithelial and mucosal surfaces, causing painful lesions and considerable emotional stress (Whitley, 1990). It is well known that, coincident with acute herpes infection, the virus enters the nervous system and that viral latency and the potential for reactivation and recurrent disease are a lifelong threat (Mertz, 1990; Roizman and Kaplan, 1992).

Many years ago, we developed the first effective antiviral for the topical treatment of ocular HSV-1 infection (Kaufman, 1962; Kaufman and Maloney, 1962; Kaufman et al., 1962). Since then, numerous anti-herpetic drugs have been designed and tested; the current armamentarium includes thymidine analogs, arabinonucleosides, and various acyclonucleosides (Elion, 1985; Beyer et al., 1989; Mansuri and Martin, 1991; Lapucci et al., 1993). Virtually all of the drugs that are presently available shorten the duration of acute herpes infection of end organs such as the ocular surface and the genital tract.

A major goal in antiviral drug development is the design of chemotherapeutic agents that specifically inhibit viral reactivation from latency. Because HSV-1 achieves latency in the nervous system and because reactivation from latency depends on certain viral enzymes, many investigators have sought to target virally encoded enzymes with drugs that inactivate or compete with viral synthetic mechanisms (Elion, 1985; Leib et al., 1990; Nsiah et al., 1990; Kaufman et al., 1991; Bourne et al., 1992; Lapucci et al., 1993; Taylor et al., 1994). Viral thymidine kinase has been widely studied in this regard (Nutter et al., 1987; Martin et al., 1989a,b; Spadari and Wright, 1989; Klein and Czelusniak, 1990; Kim et al., 1993), and the status of inhibitors of this enzyme has been reviewed (Wright, 1994). Inhibitors of HSV thymidine kinase were first proven to be effective in preventing viral reactivation in an in vitro explant-cocultivation model of latently infected murine trigeminal ganglia (Leib et al., 1990).

Some of the currently available chemotherapeutic agents have been shown to be effective in reducing HSV-1 and HSV-2 recurrences in very specific circumstances (Park et al., 1979; Saral et al., 1981; Straus et al., 1984; Douglas et al., 1984; Meyrick Thomas et al., 1985, Spruance et al., 1988; Rooney et al., 1993). For example, acyclovir is effective in reducing the viral recurrence rate in patients with urogenital HSV-2 infection (Corey et al., 1982; Douglas et al., 1984; Mindel et al., 1984, 1988; Straus et al., 1984; Gold and Corey, 1987). Similarly, acyclovir is effective in reducing the frequency of recurrences of oral–facial HSV-1 (Spruance et al., 1988; Rooney et al., 1993). Unfortunately, neither systemic nor topical acyclovir has been proven effective in preventing ocular recurrences of HSV-1 infection (Sanitato et al., 1984; Collum et al., 1986). Barney and Foster (1994) found that acyclovir reduced the recurrence rate of ocular herpes after keratoplasty, but steroids were used after the surgery and antivirals are known to reduce recurrence rates after topical corticosteroid administration. Legmann and Langston (1995) presented a non-randomized, retrospective study of a small group of patients who seemed to have fewer recurrences when given oral acyclovir, and there is an NIH-sponsored study (Herpetic Eye Disease Study) in progress to determine if oral acyclovir is useful in preventing herpetic recurrences. To date, however, there are no conclusive data that establish the value of acyclovir in preventing ocular herpetic recurrences in patients who are not treated with steroids.

Recently, we have been successful in synthesizing a compound that potently and specifically inhibits herpetic viral thymidine kinases (Xu et al., 1995). This compound, 9-(4-hydroxybutyl)-N^2-phenylguanine (HBPG), has physicochemical properties that make it suitable for testing in vivo. HBPG has been found to be active in preventing HSV-1 reactivation in a mouse model of heat stress-induced reactivation (Gebhardt et al., 1996). Using our recently described primate model of hypothermic induction of HSV-1 reactivation (Varnell et al., 1995), we tested HBPG for the ability to reduce ocular recurrences of herpetic keratitis in monkeys.

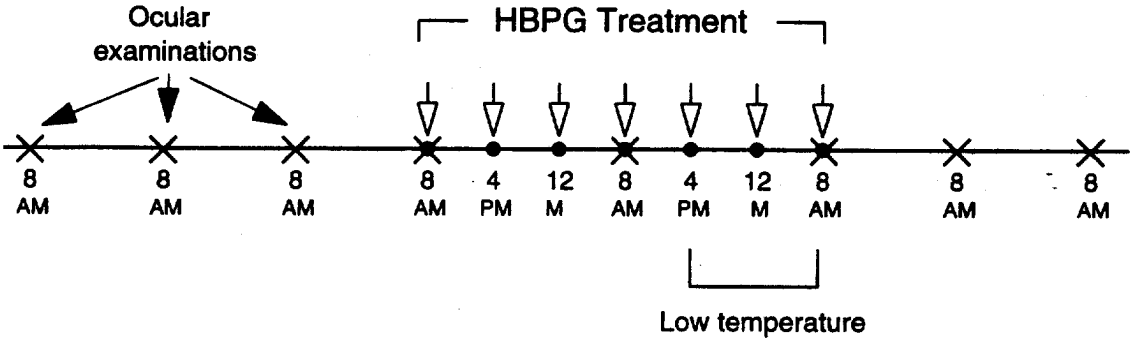

Fig. 1. Diagram of experimental design. Monkeys were treated every 8 h with i.p. injection of 150 mg/kg HBPG or corn oil. At the time of the fifth injection, the ambient temperature was reduced to 16–18°C for a period of 16 h, during which time two additional treatments were given. Eyes were examined every morning at 08:00 (X) for several days before, during, and several days after the period of hypothermic stress (see Fig. 3).

2. Materials and methods

2.1. Animals

Eighteen male or female young adult squirrel monkeys (*Saimiri scuireus*) weighing 0.46–1.08 kg were used. All animals were handled in accordance with the NIH guidelines on the care and use of animals in research, the Association for Research in Vision and Ophthalmology Statement for the Use of Animals in Ophthalmic and Vision Research, and the approval of the Institutional Animal Care and Use Committee of the LSU Medical Center in New Orleans. The monkeys had previously been used in breeding research but had not been involved in any infectious disease research.

2.2. Pharmacokinetic studies

Four monkeys were given single i.p. injections of 150 mg/kg HBPG in corn oil suspension (10 mg/ml) and bled 2, 5, 8 and 10 h later. Two monkeys were given single intravenous (i.v.) injections of 40 mg/kg HBPG dissolved in 90% dimethylsulfoxide (10 mg/ml), and bled 0.5, 1, 2 and 3 h later. The primates were anesthetized with 10–40 mg/kg intramuscular ketamine prior to injection of the drug, and were reanesthetized as necessary for phlebotomy from the femoral vein. No more than 0.2 ml of blood was removed at each time point. Plasma was separated, frozen, and subjected to analysis for HBPG content. Diluted plasma samples were analyzed by high-performance liquid chromatography (HPLC) on a C8 reverse-phase column, and concentrations of HBPG were calculated from the absorbance of the compound at 275 nm. Details of the conditions have been published (Xu et al., 1995).

2.3. Efficacy trial

The corneas of the 18 squirrel monkeys were anesthetized with a drop of proparacaine hydrochloride (Alcaine, Alcon, Humacao, PR). The superficial corneal epithelium was minimally traumatized with a 27-gauge needle, after which 25 μl of Rodanus strain HSV-1 was dropped into the conjunctival cul-de-sac, and the eyelids were gently rubbed over the cornea for 10 s. The corneas were stained with fluorescein (Fluor-I-Strip, Wyeth-Ayerst, Philadelphia, PA) 3 days after infection and the presence of herpetic keratitis was verified in all corneas by slit-lamp biomicroscopic examination. Based on the pharmacokinetic data, we decided to use 150 mg/kg HBPG, i.p. every 8 h, and to inject drug or vehicle a total of five times before lowering the room temperature.

Fig. 1 illustrates the experimental design. To induce recurrences with hypothermic stress, the room temperature was lowered at 16:00. Drug treatment was continued two additional times

(midnight and 08:00), and the desired low temperature was noted at 06:00. Corneas were examined at 08:00, and the room temperature was raised to the normal level. Animals were exposed to four cycles of temperature stress, with treatments starting on days 21, 27, 34 and 69. A cross-over study was not undertaken in order to avoid any drug carryover from a possible depot of drug that might slowly dissolve. Each animal was followed serially because it is known that the numbers of recurrences decrease with time after infection. The corneal evaluations were done in a masked manner so that the observer had no knowledge of the treatments.

2.4. Statistical methods

The outcome was expressed as a binary variable with the value 1 if an eye had a typical herpetic lesion, 0 if it did not. The dependent variable was the treatment, either HBPG or the vehicle. The analyses were conducted separately for the time during treatment and the time of no treatment. The analysis was a Wilcoxon rank sums test using a correction for a normal approximation with a continuity correction for the two sample case (i.e. the two levels of the treatment, HBPG and the vehicle (Siegel, 1956)).

3. Results

Plasma from HBPG-treated animals was analyzed by HPLC to measure the time course of drug residence in the circulation. The results of i.v. dosing (Fig. 2(A)) showed an elimination half-life of 1.05 h and a volume of distribution, 0.83 l/kg, that indicated uniform distribution of the drug throughout body tissues. By contrast, after i.p. injection, HBPG had an apparent plasma half-life of 12.5 h (Fig. 2(B)), indicating that elimination of the drug was dependent on the absorption rate from the peritoneal cavity. The prolonged plasma half-life suggested that i.p. injection at convenient dosing intervals would provide adequate and consistent concentrations of drug at the target site, the trigeminal ganglion. Intravenous dosing would have been impossible, given the short half-life of the administered drug and the volume of fluids required for i.v. administration in such small animals. Indeed, the dosing frequency by the i.p. route was chosen in order to achieve higher peak drug concentrations at steady state than was possible with a single dose.

The dosing frequency was chosen to cause a degree of cumulation of drug in the plasma at

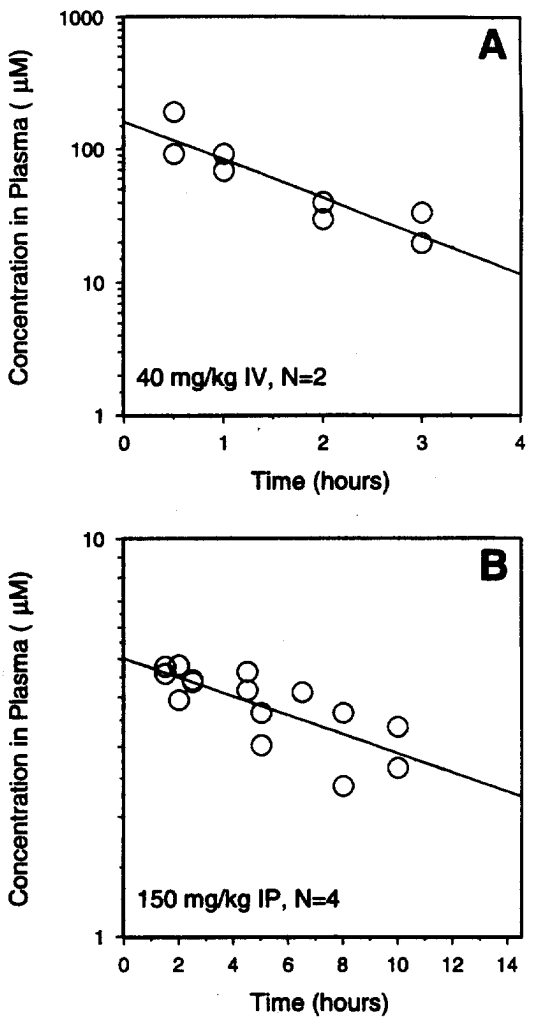

Fig. 2. (A) Plasma concentration of HBPG in two squirrel monkeys that had been given a single i.v. injection of 40 mg/kg HBPG dissolved in 90% dimethylsulfoxide shows an elimination half-life of 1.05 h and a volume of distribution of 0.83 l/kg. (B) Plasma concentration of HBPG in four squirrel monkeys that had been given a single i.p. injection of 150 mg/kg HBPG in corn oil shows an apparent half-life of 12.5 h.

Table 1
Recurrent epithelial herpetic keratitis in squirrel monkeys infected with HSV-1 strain Rodanus

Treatment[a]	No. of observations[b]	Eyes		Eye lesion days
		Recurrent lesions	No recurrent lesions	
Corn oil	432	9/18	9/18	47
HBPG	372	10/18	8/18	19

[a] HBPG 150 mg/kg i.p. every 8 h on PI days 21, 22, 27, 28, 34, 35, 69, 70, 71 and 72, and at 08:00 on PI days 23, 29, 36 and 73; corn oil given i.p. on same schedule.
[b] Total eyes examined over all days of study (PI days 16–73).

steady state and to reduce the peak-to-trough variation during the reactivation protocol. By beginning drug treatments before lowering the temperature, the plasma concentration of drug would be near steady state (about 4 half-lives). Assuming that the plasma concentration just before the next dose, a, is given by $a = b \exp(-0.693/t^{1/2})t$, where b is the peak concentration and t is the dosing interval, the extent of cumulation with a dosing frequency of 8 h is 2.8, i.e. $b/(b-a)$. Thus, the peak plasma concentration at steady state would be 14 μM (2.8 × 5 μM (see Fig. 2(B)) and the trough would be 9 μM.

All nine monkeys randomized to the HBPG-treated group and six of the nine monkeys randomized to the vehicle-treated group had at least one incident of recurrent herpetic keratitis during the observation period (Table 1 and Fig. 3). During the treatment periods, the frequency of corneas showing specific recurrent herpetic keratitis was significantly lower in the HBPG-treated group than in the untreated control group ($P = 0.01$, Wilcoxon rank sums test). In the periods before and after treatment, there were no significant differences in the frequency of herpetic keratitis between the two treatment groups (before: $P = 0.6536$; after: $P = 0.1106$).

Three monkeys died during the study, one on the night of day 28 when the temperature was lowered to 16°C, one on the night of day 34, and one during the night of day 69. Although all three events were associated with treatment periods (6, 3, and 3 consecutive doses, respectively), the veterinarian who performed the post mortem examinations did not find any gross or histologic findings suggesting HBPG toxicity. He found non-specific changes suggesting hypoglycemia/shock/possible stroke that could have been related to the low temperature. Further studies of drug toxicity will be required in the future.

4. Discussion

It is essential to demonstrate the safety and efficacy of drugs that target viral enzyme systems in primate species before testing these drugs in the clinical setting. In the present study, we used a model of hypothermic stress in primates (Varnell et al., 1995). In this model, latently infected squirrel monkeys subjected to brief intervals of lowered ambient temperatures (to approximately 18°C) exhibited a significantly greater number of corneal herpetic lesions compared with latently infected animals maintained in an ambient temperature range of 24–27°C. The results of the present study provide evidence that a new drug, HBPG, which inhibits viral thymidine kinase, is effective in preventing viral reactivation and recrudescence of ocular viral disease in hypothermically stressed primates. These results support and broaden our previous investigations with this and related compounds (Xu et al., 1995; Gebhardt et al., 1996).

Xu et al. (1995) demonstrated that HBPG is an effective inhibitor of HSV-1 thymidine kinase in vitro and provided convincing evidence that this compound achieves effective systemic distribution and plasma levels, making it an ideal candidate for further study as an antiviral. Subsequently, Gebhardt et al. (1996) showed that HBPG is effective in reducing viral reactivation in a murine model; they demonstrated a reduced frequency of

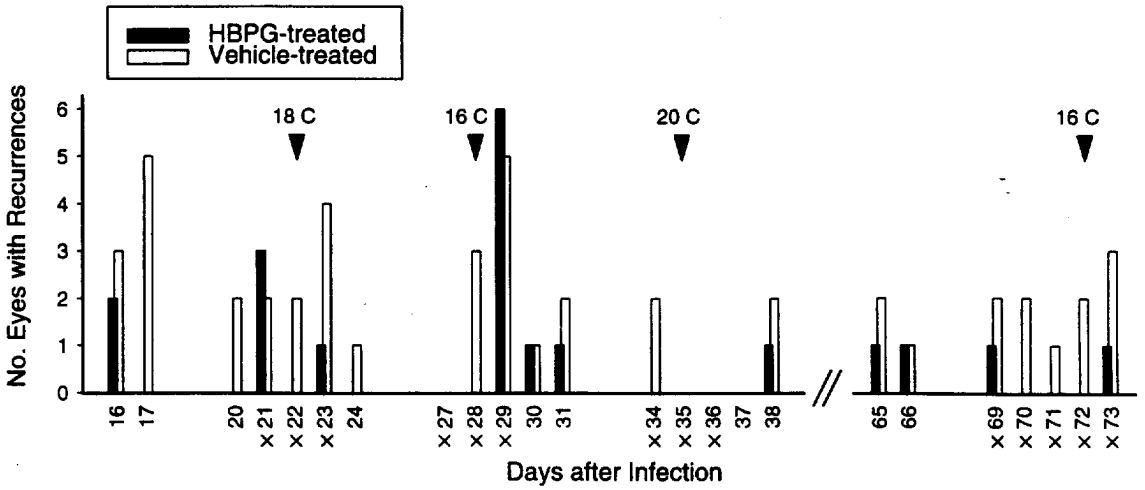

Fig. 3. The animals were examined only on the numbered days after infection; they were not examined on weekends or during the period of post-infection (PI) day 39 through PI day 64. X denotes days of treatment. Vehicle-treated group = nine monkeys (18 eyes). HBPG-treated group = nine monkeys (18 eyes) through PI day 28, eight monkeys (16 eyes) through PI day 34, seven monkeys (14 eyes) through PI day 69, and six monkeys (12 eyes) to end of study. On PI day 35, the room temperature could not be lowered to the desired range of 16–18°C; a low of 20°C was attained. On PI days 35, 36 and 37, no recurrent keratitis was seen in either group.

ocular shedding of infectious virus, as well as reduced synthesis of viral DNA in the trigeminal ganglion, the site of viral latency, in HBPG-treated animals compared with untreated controls. In the present study, however, corneas were not cultured for the presence of herpesvirus because swabbing the eyes can damage the cornea and cause other trauma which may mimic viral lesions or perhaps even induce viral shedding.

Research into antiviral drugs has been focused on compounds that shorten the duration of acute infection and the destructive effects of the virus in the infected organs (Elion, 1985; Beyer et al., 1989; Mansuri and Martin, 1991; Lapucci et al., 1993). For HSV-1 and HSV-2, a major thrust of drug development is aimed at preventing viral reactivation. An especially desirable goal is to develop a safe, nontoxic, effective antiviral that can be self-administered and that can prevent viral reactivation in carriers of latent herpesviruses. For many years, we have focused our attention on the design and testing of antiviral compounds directed against metabolic pathways that are involved in viral synthesis and assembly during reactivation from latency (Kaufman, 1993), and we believe that viral thymidine kinase inhibitors that do not affect host enzymes have great potential for both safety and efficacy. For example, we tested the thymidine kinase inhibitor 5′-ethynylthymidine and found that this drug suppressed ocular recurrences of HSV-1 (Kaufman et al., 1991). Unfortunately, in order to achieve the desired effect, the drug had to be administered i.p. every 4 h for many days. Our present study with HBPG in primates provides a stimulus for further investigation into the use of such compounds in preventing viral reactivation in the clinical setting. Ultimately, it should be possible to provide patients with an oral medication that can be taken routinely in circumstances where viral reactivation is a likely event.

Acknowledgements

This work was supported in part by US Public Health Service grants EY02672, EY02377 and EY08701 from the National Eye Institute, National Institutes of Health, Bethesda, MD, Department of the Army, Cooperative Agreement

DAMD17-93-V-3013 (this does not necessarily reflect the position or the policy of the government, and no official endorsement should be inferred), as well as an unrestricted departmental grant (LSU Eye Center) from Research to Prevent Blindness, New York, NY. This study was presented in part at the 8th International Conference on Antiviral Research, Santa Fe, NM, April 24, 1995.

References

Barney, N.P. and Foster, C.S. (1994) A prospective randomized trial of oral acyclovir after penetrating keratoplasty for herpes simplex keratitis. Cornea 13, 232–236.

Beyer, C.F., Hill, J.M. and Kaufman, H.E. (1989) Antivirals and interferons. Ophthalmol. Clin. North Am. 2, 51–63.

Bourne, N., Bravo, F.J., Ashton, W.T., Meurer, L.C., Tolman, R.L., Karkas, J.D. and Stanberry, L.R. (1992) Assessment of a selective inhibitor of herpes simplex virus thymidine kinase (L-653,180) as therapy for experimental recurrent genital herpes. Antimicrob. Agents Chemother. 36, 2020–2024.

Collum, L.M.T., McGettrick, P., Akhtar, J., Lavin, J. and Rees, P.J. (1986) Oral acyclovir (Zovirax) in herpes simplex dendritic corneal ulceration. Br. J. Ophthalmol. 70, 435–438.

Corey, L., Nahmias, A.J., Guinan, M.E., Benedetti, J.K., Critchlow, C.W. and Holmes, K.K. (1982) A trial of topical acyclovir in genital herpes simplex virus infections. N. Engl. J. Med. 306, 1313–1319.

Douglas, J.M., Critchlow, C., Benedetti, J., Mertz, G.J., Connor, J.D., Hintz, M.A., Fahnlander, A., Remington, M., Winter, C. and Corey, L. (1984) A double-blind study of oral acyclovir for suppression of recurrences of genital herpes simplex virus infection. N. Engl. J. Med. 310, 1551–1556.

Elion, G.B. (1985) Selectivity — key to chemotherapy: presidential address. Cancer Res. 45, 2943–2950.

Gebhardt, B.M., Wright, G.E., Xu, H., Focher, F., Spadari, S. and Kaufman, H.E. (1996) 9-(4-hydroxybutyl)-N^2-phenylguanine. HBPG, a thymidine kinase inhibitor, suppresses herpes virus reactivation in vivo. Antiviral Res. 30, 87–94.

Gold, D. and Corey, L. (1987) Acyclovir prophylaxis for herpes simplex virus infection. Antimicrob. Agents Chemother. 31, 361–367.

Kaufman, H.E. (1962) Clinical cure of herpes simplex keratitis by 5-iodo-2′-deoxyuridine. Proc. Soc. Exp. Biol. Med. 109, 251–252.

Kaufman, H.E. (1993) Introduction: the first effective antiviral. In: J. Adams and V.J. Merluzzi (Eds), The Search for Antiviral Drugs, pp. 1–21. Birkhäuser, Boston.

Kaufman, H.E. and Maloney, E.D. (1962) IDU and hydrocortisone in experimental herpes simplex keratitis. Arch. Ophthalmol. 68, 396–398.

Kaufman, H.E., Nesburn, A.B. and Maloney, E.D. (1962) IDU therapy of herpes simplex. Arch. Ophthalmol. 67, 583–591.

Kaufman, H.E., Varnell, E.D., Cheng, Y.C., Bobek, M., Thompson, H.W. and Dutschman, G.E. (1991) Suppression of ocular herpes recurrences by a thymidine kinase inhibitor in squirrel monkeys. Antiviral Res. 16, 227–232.

Kim, C.U., Misco, P.F., Luh, B.Y., Terry, B., Bisacchi, G. and Mansuri, M.M. (1993) (2*R*,4*S*,5*S*)-1-(tetrahydro-4-hydroxy-5-methoxy-2-furanyl)thymine: a potent selective inhibitor of herpes simplex thymidine kinase. Bioorg. Med. Chem. 3, 1571–1576.

Klein, R.J. and Czelusniak, S.M. (1990) Effect of a thymidine kinase inhibitor (L-653,180) on antiviral treatment of experimental herpes simplex virus infection in mice. Antiviral Res. 14, 207–214.

Lapucci, A., Macchia, M. and Parkin, A. (1993) Antiherpes virus agents: a review. Farmaco 48, 871–895.

Legmann, A. and Langston, D.P. (1995) Long-term oral acyclovir therapy: effect on recurrent infectious herpes simplex keratitis. Ophthalmology 102 (Suppl. 9A), 121.

Leib, D.A., Ruffner, K.L., Hildebrand, C., Schaffer, P.A., Wright, G.E. and Coen, D.M. (1990) Specific inhibitors of herpes simplex virus thymidine kinase diminish reactivation of latent virus from explanted murine ganglia. Antimicrob. Agents Chemother. 34, 1285–1286.

Mansuri, M.M. and Martin, J.C. (1991) Antiviral agents. Annu. Rep. Med. Chem. 26, 133–140.

Martin, J.A., Duncan, I.B. and Thomas, G.J. (1989a) Design of inhibitors of herpes simplex virus thymidine kinase. In: J.C. Martin (Ed), Nucleotide Analogues as Antiviral Agents, pp. 103–115. American Chemical Society, Washington, D.C.

Martin, J.A., Duncan, I.B., Hall, M.J., Wong-Kai-In, P., Lambert, R.W. and Thomas, G.J. (1989b) New potent and selective inhibitors of herpes simplex virus thymidine kinase. Nucleosides Nucleotides 8, 753–764.

Mertz, G.J. (1990) Herpes simplex virus. In: G.J. Galasso, R.J. Whitley and T.C. Merigan (Eds), Antiviral Agents and Viral Diseases of Man, 3rd Edn., pp. 265–300. Raven Press, New York.

Meyrick Thomas, R.H., Dodd, H.J., Yeo, J.M. and Kirby, J.D.T. (1985) Oral acyclovir in the suppression of recurrent non-genital herpes simplex virus infection. Br. J. Dermatol. 113, 731–735.

Mindel, A., Weller, I.V.D., Faherty, A., Sutherland, S., Hindley, D., Fiddian, A.P. and Adler, M.W. (1984) Prophylactic oral acyclovir in recurrent genital herpes. Lancet i, 57–59.

Mindel, A., Faherty, A., Carney, O., Patou, G., Freris, M., Williams, P. (1988) Dosage and safety of long-term suppressive acyclovir therapy for recurrent genital herpes. Lancet i, 926–928.

Nsiah, Y.A., Tolman, R.L., Karkas, J.D. and Rapp, F. (1994) Suppression of herpes simplex virus type 1 reactivation from latency by (±)-9-{[(*Z*)-2-(hydroxymethyl)cyclohexyl]methyl}guanine (L-653,180) in vitro. Antimicrob. Agents Chemother. 34, 1551–1555.

Nutter, L.M., Grill, S.P., Dutschman, G.E., Sharma, R.A., Bobek, M. and Cheng, Y.-C. (1987) Demonstration of viral thymidine kinase inhibitor and its effect on deoxynucleotide metabolism in cells infected with herpes simplex virus. Antimicrob. Agents Chemother. 31, 368–374.

Park, N.H., Pavan-Langston, D. and McLean, S.L. (1979) Acyclovir in oral and ganglionic herpes simplex virus infections. J. Infect. Dis. 140, 802–806.

Roizman, B. and Kaplan, L.J. (1992) Herpes simplex viruses, central nervous system, and encephalitis. A two-body problem, with one outcome and too many questions. In: R.P. Roos (Ed), Molecular Neurovirology, pp. 3–21. Humana Press, Totowa, NJ.

Rooney, J.F., Straus, S.E., Mannix, M.L., Wohlenberg, C.R., Alling, D.W., Dumois, J.A. and Notkins, A.L. (1993) Oral acyclovir to suppress frequently recurrent herpes labialis. A double-blind, placebo-controlled trial. Ann. Intern. Med. 118, 268–272.

Sanitato, J.J., Asbell, P.A., Varnell, E.D., Kissling, G.E. and Kaufman, H.E. (1984) Acyclovir in the treatment of herpetic stromal disease. Am. J. Ophthalmol. 98, 537–547.

Saral, R., Burns, W.H., Laskin, O.L., Santos, G.W. and Lietman, P.S. (1981) Acyclovir prophylaxis of herpes-simplex-virus infections. A randomized, double-blind, controlled trial in bone-marrow-transplant recipients. N. Engl. J. Med. 305, 63–67.

Siegel, S. (1956) Nonparametric Statistics for the Behavioral Sciences, 312 pp. Ch. 5. The case of two related samples. The Wilcoxon matched-pairs signed ranks test, pp. 75–78. McGraw-Hill, New York.

Spadari, S. and Wright, G. (1989) Antivirals based on inhibition of herpesvirus thymidine kinases. Drug News Perspectives 2, 333–336.

Spruance, S.L., Hamill, M.L., Hoge, W.S., Davis, L.G. and Mills, J. (1988) Acyclovir prevents reactivation of herpes simplex labialis in skiers. J. Am. Med. Assoc. 260, 1597–1599.

Straus, S.E., Takiff, H.E., Seidlin, M., Bachrach, S., Lininger, L., DiGiovanna, J.J., Western, K.A., Smith, H.A., Lehrman, S.N., Creagh-Kirk, T. and Alling, D.W. (1984) Suppression of frequently recurring genital herpes: a placebo-controlled double-blind trial of oral acyclovir. N. Engl. J. Med. 310, 1545–1550.

Straus, S.E. (moderator), Rooney, J.F., Sever, J.L., Seidlin, M., Nusinoff-Lehrman, S. and Cremer, K. (discussants) (1985) Herpes simplex virus infection: biology, treatment, and prevention. NIH Conference. Ann. Intern. Med. 103, 404–419.

Taylor, J.L., Tom, P., Guy, J., Selvarajan, R.M. and O'Brien, W.J. (1994) Regulation of herpes simplex virus thymidine kinase in cells treated with a synergistic antiviral combination of alpha interferon and acyclovir. Antimicrob. Agents Chemother. 38, 853–856.

Varnell, E.D., Kaufman, H.E., Hill, J.M. and Thompson, H.W. (1995) Cold stress-induced recurrences of herpetic keratitis in the squirrel monkey. Invest. Ophthalmol. Vis. Sci. 36, 1181–1183.

Whitley, R.J. (1990) Herpes simplex viruses. In: B.N. Fields, D.M. Knipe, R.M. Chanock, M.S. Hirsch, J.L. Melnick, T.P. Monath and B. Roizman (Eds), Virology, 2nd Edn., pp. 1843–1887. Raven Press, New York.

Wright, G.E. (1994) Herpesvirus thymidine kinase inhibitors. Int. Antiviral News 2, 84–86.

Xu, H., Maga, G., Focher, F., Smith, E.R., Spadari, S., Gambino, J. and Wright, G.E. (1995) Synthesis, properties, and pharmacokinetic studies of N^2-phenylguanine derivatives as inhibitors of herpes simplex virus thymidine kinases. J. Med. Chem. 38, 49–57.

Archives of Ophthalmology: Clinical Sciences Section

Date submitted: October 14, 1997

Trifluridine, Cidofovir, and Penciclovir in the Treatment of Experimental Herpetic Keratitis

Herbert E. Kaufman, MD; Emily D. Varnell, BS; Hilary W. Thompson, PhD

From the LSU Eye Center, Louisiana State University Medical Center School of Medicine, New Orleans, Louisiana

Proprietary Interests: Cidofovir powder was supplied by Gilead Scientific, Foster City, California. Penciclovir powder was supplied by SmithKline Beecham, King of Prussia, Pennsylvania. None of the authors have any financial interest in or receive payment as a consultant, reviewer, or evaluator from either company.

Correspondence and reprint requests to: Emily D. Varnell, LSU Eye Center, 2020 Gravier Street, Suite B, New Orleans, LA 70112-2234. Phone 504-568-6700 ext 336; fax 504-568-4210. E-mail EVARNE@LSUMC.EDU

ABSTRACT

Purpose: To compare trifluridine eye drops, cidofovir eye drops, and penciclovir ophthalmic ointment for the treatment of herpes simplex virus type 1 (HSV-1) keratitis.

Methods: New Zealand white rabbits were infected with the McKrae strain of HSV-1. Three days after virus inoculation, the rabbits were randomized to treatment with either 1% trifluridine, 0.2% cidofovir, 3% penciclovir ointment, or phosphate-buffered saline (PBS; control) on various schedules. The severity of keratitis was graded in a masked fashion.

Results: Treatment with any of the antiviral drugs resulted in significantly less severe keratitis than treatment with PBS. There was no statistically significant difference between eyes given trifluridine two, four, or seven times a day and eyes given cidofovir two times a day ($P=.056$, $P=.426$, $P=.189$ respectively, F-test, ANOVA).Cidofovir twice a day was significantly more effective than penciclovir given either two or four times a day ($P=.0001$, $P=.002$ respectively). Even with once-a-day dosage, all three drugs were significantly more effective than PBS ($P=.0001$ for all). There was no significant difference between once-a-day trifluridine and cidofovir treatments ($P=.1692$). Trifluridine administered five times a day was as effective as 1% cidofovir.

Conclusions: Trifluridine was highly effective in this rabbit model, even when given only once a day. Cidofovir was as effective as trifluridine. Cidofovir and penciclovir may prove to be effective treatments for epithelial keratitis, and clinical trials of the three drugs with lower treatment frequencies appear to be warranted.

The rabbit provides a model of HSV keratitis that involves the multiplication of HSV in the rabbit corneal epithelium with the production of dendrites and is similar to the infection in humans. Studies using this model have been predictive of results in humans, and the relative potencies of drugs determined in this model have paralleled those seen in human studies.[1-4] The purpose of our study was to compare two of the newer antiviral drugs, penciclovir and cidofovir, with trifluridine, which one of us (H.E.K.) introduced as an effective antiviral 34 years ago,[3] and to determine the frequency of drug administration needed for effective therapy. There are theoretical reasons suggesting that these newer drugs may persist for a longer period of time in ocular tissues and could, therefore, be administered less frequently than trifluridine.

Trifluridine is a substituted nucleoside similar to thymidine.[5] For the drug to become active, it must be phosphorylated by cellular thymidine kinase (a relatively rate limiting step), and then additionally phosphorylated by the more rapidly acting cellular enzymes. The primary action of trifluridine is inhibition of DNA polymerase; it may also act within the cell to block the synthesis of thymidilic synthetase. As approved by the Food and Drug Administration (FDA), the package insert suggests application of one drop of trifluridine every 2 hours during waking hours, up to a maximum daily dosage of nine drops. Trifluridine has been found to inhibit the growth of adenovirus in tissue culture.

Penciclovir (9-[4-hydroxy-3-hydroxymethylbut-1-yl]guanine) (and its better absorbed oral prodrug, famciclovir, which is hydrolyzed to penciclovir) is a nucleoside similar to acyclovir. Famciclovir has been approved by the FDA for use in treating herpes zoster and appears to reduce post-zoster pain.[6] Like trifluridine, penciclovir is initially phosphorylated by cellular thymidine kinase and then rapidly phosphorylated to the triphosphate.[7] Also like

trifluridine, penciclovir is an inhibitor of DNA polymerase, but it is more selective than trifluridine. Although the active triphosphate of penciclovir is somewhat less inhibitory toward DNA polymerase than the acyclovir triphosphate, penciclovir persists in the cell for a significantly longer period of time and, therefore, requires less frequent administration. For this reason, it seemed like a good candidate for a long-acting topical antiviral.

Cidofovir (1-[(S)-3-hydroxy-2-(phosphonomethoxy)propyl]cytosine; HPMPC), unlike trifluridine and penciclovir, is a phosphonate. Like foscarnet, cidofovir already has the first phosphate in place and then rapidly acquires two additional phosphates without the need for thymidine kinase.[8,9] Phosphonates inhibit DNA polymerase, but changes in thymidine kinase do not cause resistance to develop.[10] Cidofovir is significantly toxic when given in high concentrations and when given frequently as a topical medication, and it is highly nephrotoxic when given systemically.[11] To be used systemically, cidofovir requires concomitant administration of probenecid to reduce active secretion of the drug into the renal tubules. Like penciclovir, cidofovir also seems to persist in tissues for a long time.[12-15]

The purpose of this study was to compare the effectiveness of these three drugs -- trifluridine, cidofovir, and penciclovir -- in a variety of dosage regimens for the treatment of herpes keratitis in the rabbit eye.

MATERIALS AND METHODS

New Zealand white rabbits (2-3 kg) of both sexes were used. All animals were handled in accordance with the NIH guidelines on the care and use of animals in research, the Louisiana State University Medical Center Institutional Animal Care and Use Committee

guidelines and approvals, and the Association for Research in Vision and Ophthalmology Statement for the Use of Animals in Ophthalmic and Vision Research.

Drugs used in this study included 1% trifluridine drops (Viroptic, Glaxo Wellcome, Research Triangle Park, North Carolina), 0.2% or 1% cidofovir solution formulated in our laboratory from cidofovir powder supplied by Gilead Scientific (Foster City, California), and 3% penciclovir ointment formulated in our laboratory from powder supplied by SmithKline Beecham (King of Prussia, Pennsylvania). Control eyes were treated with phosphate-buffered saline (PBS).

HSV-1 strain McKrae was propagated in primary rabbit kidney cells and titered in CV-1 cells. Rabbit corneas were anesthetized with proparacaine hydrochloride, the superficial corneal epithelium was lightly scarified with a 27-gauge needle, and 25 μl of virus suspension was dropped onto the cornea in order to synchronize the initial appearance and severity of keratitis. The lids were gently rubbed over the cornea for 15 seconds.

Three days after virus inoculation, the corneas were stained with fluorescein, and the severity of keratitis was graded on a scale of 0 to 4 as follows: 0 = normal cornea; 1 = epithelial ulceration involving 1/4 of the epithelial area; 2 = epithelial ulceration involving 1/2 of the epithelial area; 3 = epithelial ulceration involving 3/4 of the epithelial area ; 4 = total epithelial involvement. Rabbits were randomized to groups of comparable severity, and treatment was administered in a coded manner.

In one study designed to compare a variety of treatment regimens, there were six drug treatment groups consisting of 16 eyes each and one control group with 14 eyes. Eyes were graded through day 14 after inoculation. Treatments were:

trifluridine 1% drops, twice a day at 8 am and 8 pm;

trifluridine 1% drops, four times a day at 8 am, 12 noon, 4 and 8 pm;

trifluridine 1% drops, seven times a day at 8 am, 10 am, 12 noon, 2, 4, 6, and 8 pm;

cidofovir 0.2% drops, two times a day at 8 am and 8 pm;

penciclovir 3% ointment, two times a day at 8 am and 8 pm;

penciclovir 3% ointment, four times a day at 8 am, 12 noon, and 4 and 8 pm; and

phosphate-buffered saline (PBS) (control), two times a day at 8 am and 8 pm.

In a second study designed to compare the efficacy of a single daily treatment, there were three drug treatment groups and one control group consisting of 20 eyes each. Eyes were graded through day 10 after inoculation. Treatments were:

trifluridine 1% drops, once a day;

cidofovir 0.2% drops, once a day;

penciclovir 3% ointment, once a day; and

PBS control, once a day.

In both studies, treatment was given beginning after examination on postinfection day 3 through postinfection day 9. Corneas were stained with fluorescein and examined with the slit lamp daily, and the severity of keratitis was graded in a masked fashion.

A third study was undertaken to test the efficacy of a higher concentration of cidofovir eye drops utilizing 20 eyes in each group. Eyes were graded through day 7 after inoculation.

Treatment groups were:

trifluridine 1% drops, five times a day at 8 and 10:30 am, 1, 3:30, and 6 pm

cidofovir 1% drops, two times a day at 8 am and 6 pm

PBS control, two times a day at 8 am and 6 pm.

STATISTICAL ANALYSIS

The outcome variable was the severity of keratitis grade. The drug treatment regimens as described in the methods section were the dependent variable. Variability due to rabbit differences within treatments was controlled for by application of a repeated measures design in the analysis of variance (ANOVA). Comparisons between the keratitis severity score means for each drug regimen were conducted by protected t-tests on least square means derived from the ANOVA.[16] All *P* values stated were derived from these tests; the ANOVA and all subsequent comparisons of treatment means were conducted using programs and procedures from the Statistical Analysis System language.[17]

RESULTS

In the initial study, all treatments with trifluridine, cidofovir, or penciclovir resulted in statistically less severe herpetic keratitis than treatment with PBS (control) ($P=.0001$ for all comparisons, **Table 1** and **Figure 1**). Twice-a-day and four-times-a-day regimens of penciclovir were equally effective ($P=.6217$). There was no difference in the effectiveness of trifluridine given two, four, or seven times a day (twice a day vs. four times a day, $P=.2652$; twice a day vs. seven times a day, $P=.5504$; four times a day vs. seven times a day,

$P=.6048$) nor was there any difference in efficacy between cidofovir given twice a day and trifluridine given twice a day ($P=.0563$). Although all treatments were effective in promoting healing of herpetic keratitis, none prevented spontaneous recurrences, even while treatment was still continuing. All groups showed spontaneous recurrences after treatment was stopped.

Once-a-day treatment with trifluridine, cidofovir, or penciclovir resulted in significantly less severe keratitis than treatment with PBS ($P=.0001$ for all three comparisons, **Table 2** and **Figure 2**).

Trifluridine and cidofovir treatment resulted in significantly less severe keratitis than treatment with penciclovir at all tested dosage schedules (trifluridine twice a day vs. penciclovir twice a day, $P=.0001$; trifluridine four times a day vs. penciclovir four times a day, $P=.0212$; cidofovir twice a day vs. penciclovir twice a day, $P=.0001$).

Treatment with 1% cidofovir twice a day and 1% trifluridine five times a day resulted in rapid healing of the keratitis soon after treatment was initiated. On each study day, treatment with either drug resulted in significantly less severe keratitis than treatment with PBS ($P=.0001$); however, there was no significant difference in the severity of keratitis in eyes treated with either trifluridine or cidofovir (**Table 3** and **Figure 3**).

Mild to moderate punctate keratitis was noted with trifluridine treatment seven times a day, with all penciclovir ointment treatments, and with the 1% cidofovir treatment. The punctate keratitis appeared 4 to 5 days after the start of treatment.

COMMENT

In this model, it was possible to show that both trifluridine and cidofovir given as

infrequently as once a day were very effective for treating HSV keratitis, even with treatment beginning 72 hours after infection when the lesions were well established.[18,19] This finding suggests the possibility that trifluridine is being used clinically more frequently than is necessary. When corticosteroids are being administered, frequent dosage of trifluridine may be needed because corticosteroids reduce the antiviral effect of all these drugs. In general, however, it may be that the antivirals are being administered more frequently in clinical practice than is actually required.

The comparison studies showed that topical penciclovir is slightly less effective than trifluridine or cidofovir and seems to offer no real advantages. Cidofovir and trifluridine were equally effective against HSV keratitis and are also reported to be effective against ocular adenovirus infection.[13,20-22]

ACKNOWLEDGMENTS

This study was supported in part by United States Public Health Service grants EY02672 and EY02377 from the National Eye Institute, National Institutes of Health, Bethesda, Maryland; Department of the Army, Cooperative Agreement DAMD17-93-V-3013 (This does not necessarily reflect the position or the policy of the government, and no official endorsement should be inferred.); and an unrestricted grant to the Department of Ophthalmology from Research to Prevent Blindness, Inc., New York, New York.

Presented in part as a poster at the Association for Research in Vision and Ophthalmology Annual Meeting, Fort Lauderdale, Fla, March, 1997.

Reprints: Emily D. Varnell, BS, LSU Eye Center, 2020 Gravier Street, Suite B, New Orleans, LA 70112.

REFERENCES

1. Kaufman HE, Nesburn AB, Maloney ED. IDU therapy of herpes simplex. *Arch Ophthalmol.* 1962;67:583-591.

2. Kaufman HE, Martola E-L, Dohlman CH. The use of 5-iodo-2'-deoxyuridine (IDU) in the treatment of herpes simplex keratitis. *Arch Ophthalmol.* 1962;68:235-239.

3. Kaufman HE, Heidelberger C. Therapeutic antiviral action of 5-trifluoromethyl-2'-deoxyuridine in herpes simplex keratitis. *Science.* 1964:145;585-586.

4. Wellings PC, Awdry PN, Bors FH, Jones BR, Brown DC, Kaufman HE. Clinical evaluation of trifluorothymidine in the treatment of herpes simplex corneal ulcers. *Am J Ophthalmol.* 1972:73;932-942.

5. Heidelberger C, Parsons DG, Remy DC. Synthesis of 5-trifluoromethyluracil and 5-trifluoromethyl-2'-deoxyuridine. *J Med Chem.* 1964;7:1-5.

6. Vere Hodge RA, Sutton D, Boyd MR, Harnden MR, Jarvest RL. Selection of an oral prodrug (BRL 42810; famciclovir) for the antiherpes agent BRL 39123 [9-(4-hydroxy-3-hydroxymethylbut-1-yl)guanine; penciclovir]. *Antimicrob Agents Chemother.* 1989;33:1765-1773.

7. Boyd MR, Bacon TH, Sutton D, Cole M. Antiherpes activity of 9-(4-hydroxy-3-hydroxymethylbut-1-yl)guanine (BRL 39123) in cell culture. *Antimicrob Agents Chemother.* 1987;31:1238-1242.

8. Bronson JJ, Ghazzouli I, Hitchcock MJM, Webb RR II, Martin JC. Synthesis and antiviral activity of the nucleotide analogue (*S*)-1-[3-hydroxy-2-(phosphonylmethoxy)propyl]cytosine. *J Med Chem.* 1989;32:1457-1463.

9. De Clercq E, Sakuma T, Baba M, et al. Antiviral activity of phosphonylmethoxyalkyl derivatives of purine and pyrimidines. *Antiviral Res.* 1987;8:261-272.

10. Maudgal PC, De Clercq E. (S)-1-(3-hydroxy-2-phosphonylmethoxypropyl)cytosine in the therapy of thymidine kinase-positive and -deficient herpes simplex virus experimental keratitis. *Invest Ophthalmol Vis Sci.* 1991;32:1816-1820.

11. Lea AP, Bryson HM. Cidofovir: new drug profile. *Drugs.* 1996;52:225-230.

12. Otova B, Votruba I, Holy A. Pretreatment of the host cell with 1-(S)-(3-hydroxy-2-phosphonylmethoxypropyl)cytosine (HPMPC) is sufficient for its antiviral effect. *Acta Virol.* 1992;36:313-319.

13. Gordon YJ, Romanowski E, Araullo-Cruz T, De Clercq E. Pretreatment with topical 0.1% (S)-1-(3-hydroxy-2-phosphonylmethoxypropyl)cytosine inhibits adenovirus type 5 replication in the New Zealand rabbit ocular model. *Cornea.* 1992;11:529-533.

14. Soike KF, Huang J-L, Zhang J-Y, Bohm R, Hitchcock MJM, Martin JC. Evaluation of infrequent dosing regimens with (*S*)-1-[3-hydroxy-2-(phosphonylmethoxy-propyl]cytosine (*S*-HPMPC) on simian varicella infection in monkeys. *Antiviral Res.* 1991;16:17-28.

15. Freeman WR, Flores-Aguilar M, Huang J-S, et al. HPMPC for the long acting treatment of experimental herpes simplex retinitis in rabbits. *Invest Ophthalmol Vis Sci.* 1993;34 suppl:751.

16. Milliken GA, Johnson DE. *Analysis of Messy Data, Volume 1: Designed Experiments.* New York: Van Nostrand Reinhold;1984.

17. SAS Institute, Inc. *SAS Language Reference, Version 6,* First Edition. Cary, NC: SAS

Institute Inc; 1990.

18. Gordon YJ, Romanowski EG, Araullo-Cruz T. HPMPC, a broad-spectrum topical antiviral agent, inhibits herpes simplex virus type 1 replication and promotes healing of dendritic keratitis in the New Zealand rabbit ocular model. *Cornea.* 1994;13:516-520.

19. Gordon YJ, Romanowski EG. The relative antiviral efficacy of twice daily cidofovir versus acyclovir and trifluridine in the HSV-1/NZ rabbit keratitis model. *Invest Ophthalmology Vis Sci.* 1997;38:S724.

20. Lenette DA, Eiferman RA. Inhibition of adenovirus replication in vitro by trifluridine. *Arch Ophthalmol.* 1978;96:1662-1663.

21. Carmine AA, Brogden RN, Heel RC, Speight TM, Avery GC. Trifluridine: a review of its antiviral activity and therapeutic use in the topical treatment of viral eye infections. *Drugs.* 1982;23:329-352.

22. De Oliveira CBR, Stevenson D, LaBree L, McDonnell PJ, Trousdale MD. Evaluation of cidofovir (HPMPC, GC-504) against adenovirus type 5 infection in vitro and in a New Zealand rabbit ocular model. *Antiviral Res.* 1996;31:165-172.

FIGURE LEGENDS

Figure 1. Comparison of the severity of keratitis in rabbits infected with McKrae strain HSV-1 in both eyes and treated with one of the three drugs on various dosage schedules. Treatment was begun after the evaluation on postinfection day 3 and continued through day 9. Treatments with either 1% trifluridine drops, 0.2% cidofovir solution, or 3% penciclovir ointment were administered in a coded manner, and all grading was done in a masked manner.

Figure 2. Comparison of severity of keratitis in rabbits infected with McKrae strain HSV-1 in both eyes and treated with one of the three drugs on a once-a-day schedule. Treatment was begun after the evaluation on postinfection day 3 and continued through day 9. Treatments with either 1% trifluridine drops, 0.2% cidofovir solution, or 3% penciclovir ointment were administered once a day, in a coded manner, and all grading was done in a masked manner.

Figure 3. Comparison of severity of keratitis in rabbits infected with McKrae strain HSV-1 in both eyes and treated with 1% cidofovir twice a day or 1% trifluridine five times a day. Treatment was begun on postinfection day 3 and continued through day 7. Drug treatments were coded and all grading was done in a masked manner.

Table 1. Effect of Various Schedules of Topical Treatment on Severity of Herpetic Keratitis in the Rabbit

Treatment	No. of eyes	Severity of Keratitis* (Scale 0 to 4) on Postinfection Days 3 to 14								
		3	4	5	7	8	9	10	11	14
Trifluridine 2x/day	16	0.66 ±0.10	0.64† ±0.10	0.56† ±0.10	0.14† ±0.10	0.16† ±0.10	0.30 ±0.10	0.28 ±0.10	0.16 ±0.10	0.09 ±0.11
Trifluridine 4x/day	16	0.56 ±0.10	0.45† ±0.10	0.38† ±0.10	0.11† ±0.10	0.16† ±0.10	0.26 ±0.10	0.22 ±0.10	0.44‡ ±0.10	0.03 ±0.10
Trifluridine 7x/day	16	0.59 ±0.10	0.52† ±0.10	0.41† ±0.10	0.14† ±0.10	0.23† ±0.10	0.26 ±0.10	0.23 ±0.10	0.12 ±0.10	0.04 ±0.11
Cidofovir 2x/day	16	0.56 ±0.10	0.48† ±0.10	0.25† ±0.10	0.14† ±0.10	0.09† ±0.10	0.08 ±0.10	0.11 ±0.10	0.03 ±0.10	0.14 ±0.11
Penciclovir 2x/day	16	0.97 ±0.10	0.76† ±0.10	0.91† ±0.10	0.64† ±0.10	0.59† ±0.10	0.42 ±0.10	0.16 ±0.11	0.14 ±0.11	0.14 ±0.11
Penciclovir 4x/day	16	0.75 ±0.10	0.73† ±0.10	0.70† ±0.10	0.39† ±0.10	0.19† ±0.10	0.25 ±0.10	0.30 ±0.10	0.20 ±0.11	0.04 ±0.11
PBS 2x/day	14	0.61 ±0.11	1.21 ±0.11	2.07 ±0.11	2.17 ±0.11	0.89 ±0.11	0.14 ±0.11	0.18 ±0.11	0.04 ±0.11	0.00 ±0.13

* least square mean ± standard error or mean

† significantly better than PBS; $P < 0.05$ (Protected t-test on least square mean)

‡ significantly worse than PBS; $P < 0.05$ (Protected t-test on least square mean)

Table 2. Effect of Once-a-Day Topical Treatment on Severity of Herpetic Keratitis in the Rabbit

Treatment	No. of eyes	Severity of Keratitis* (Scale 0 to 4) on Postinfection Days 3 to 10							
		3	4	5	6	7	8	9	10
Trifluridine, 1% drops	20	0.56 ±0.12	0.64 ±0.12	0.62† ±0.12	0.81† ±0.12	0.52† ±0.12	0.36 ±0.12	0.19 ±0.12	0.07 ±0.12
Cidofovir, 0.2% drops	20	0.63 ±0.11	0.65 ±0.11	0.51† ±0.11	0.50† ±0.11	0.40† ±0.11	0.35 ±0.11	0.30 ±0.11	0.35 ±0.11
Penciclovir, 3% ointment	20	0.53 ±0.12	0.72 ±0.12	0.68† ±0.12	0.74† ±0.12	0.69† ±0.12	0.58 ±0.12	0.50 ±0.12	0.75‡ ±0.12
Phosphate-buffered saline	20	0.53 ±0.12	0.83 ±0.12	1.14 ±0.12	1.56 ±0.12	1.25 ±0.12	0.65 ±0.12	0.33 ±0.12	0.26 ±0.12

* least square mean ± standard error of the mean

† significantly better than PBS; $P < 0.05$ (Protected t-test on least square mean)

‡ significantly worse than PBS; $P < 0.05$ (Protected t-test on least square mean)

Table 3. Effect of 1% Cidofovir versus 1% Trifluridine on the Severity of Herpetic Keratitis in the Rabbit

Treatment	No. of eyes	Severity of Keratitis* on Postinfection Days 3 to 7				
		3	4	5	6	7
Trifluridine, 1% drops 5 times a day	20	0.52 ±.09	0.48† ±.09	0.05† ±.09	0.05† ±.09	0.01† ±.09
Cidofovir, 1% drops twice a day	20	0.50 ±.09	0.52† ±.09	0.09† ±.09	0.01† ±.09	0.02† ±.09
Phosphate-buffered saline twice a day	20	0.52 ±0.09	1.08 ±.09	1.88 ±.09	1.95 ±.09	1.52 ±.09

* least square mean ± standard error of the mean

† significantly better than PBS; $P = .0001$ (Protected t-test on least square mean)

Kaufman et al
Figure 1
TOP ↑

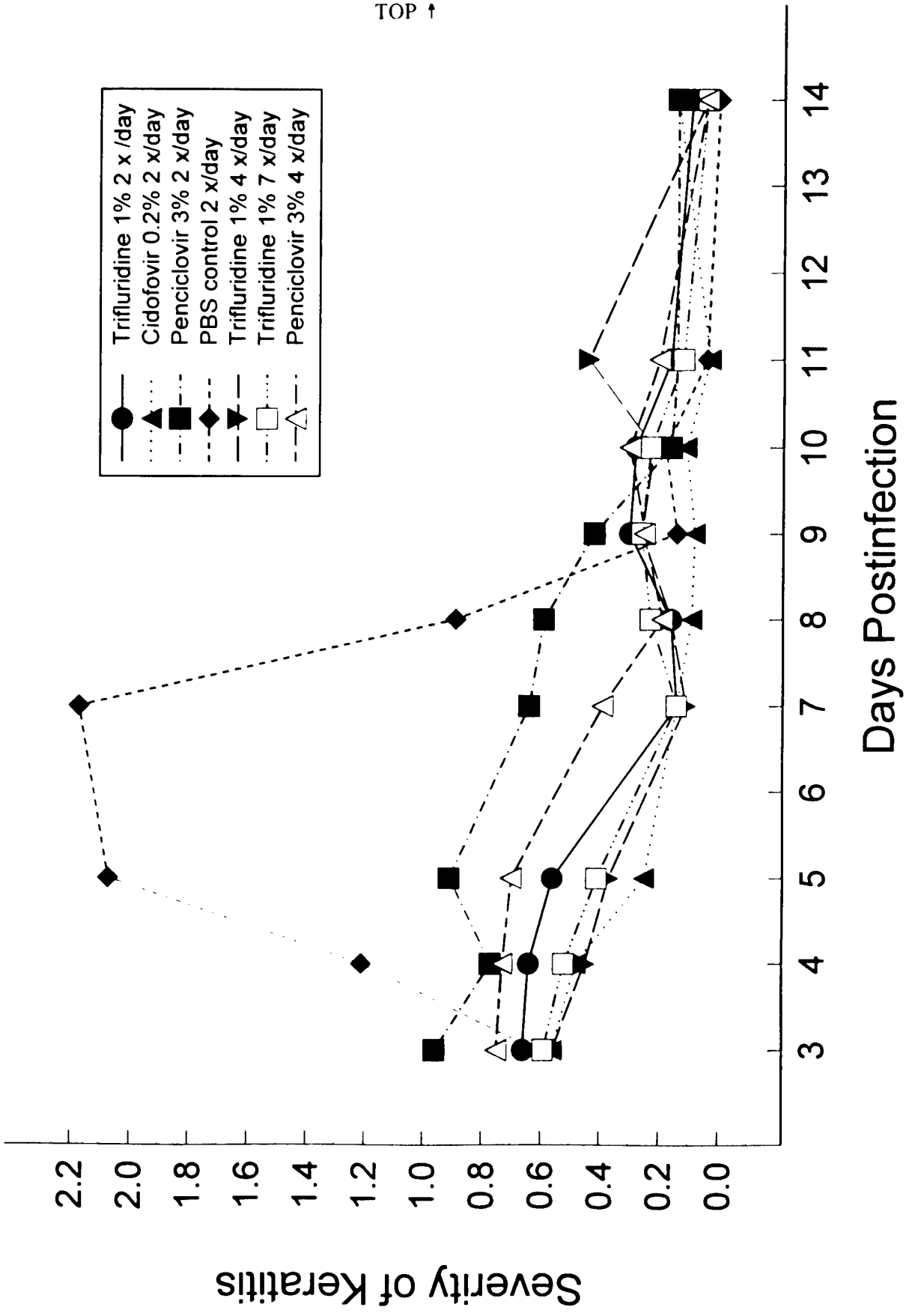

Kaufman et al
Figure 2
TOP ↑

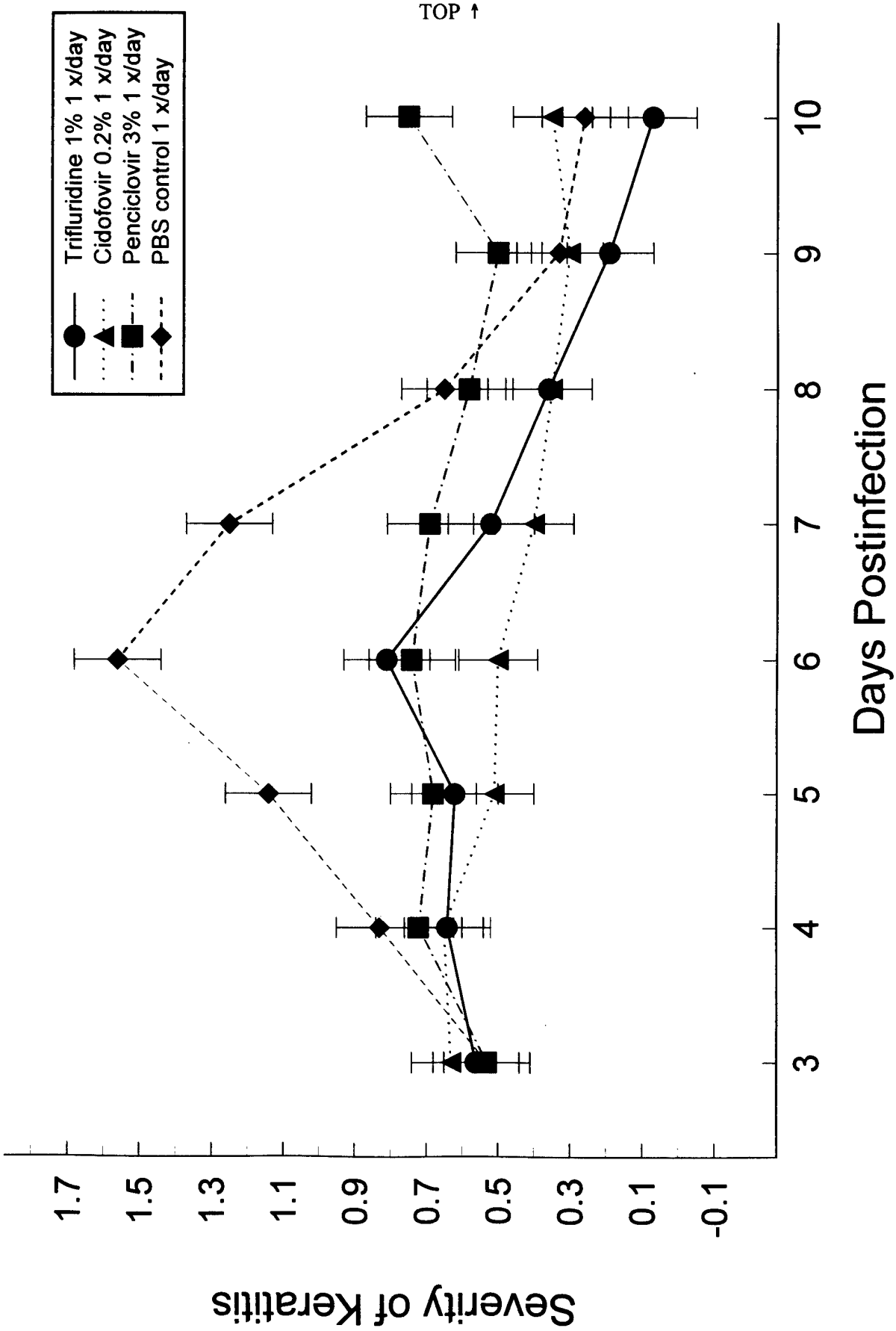

Kaufman et al
Figure 3
TOP ↑

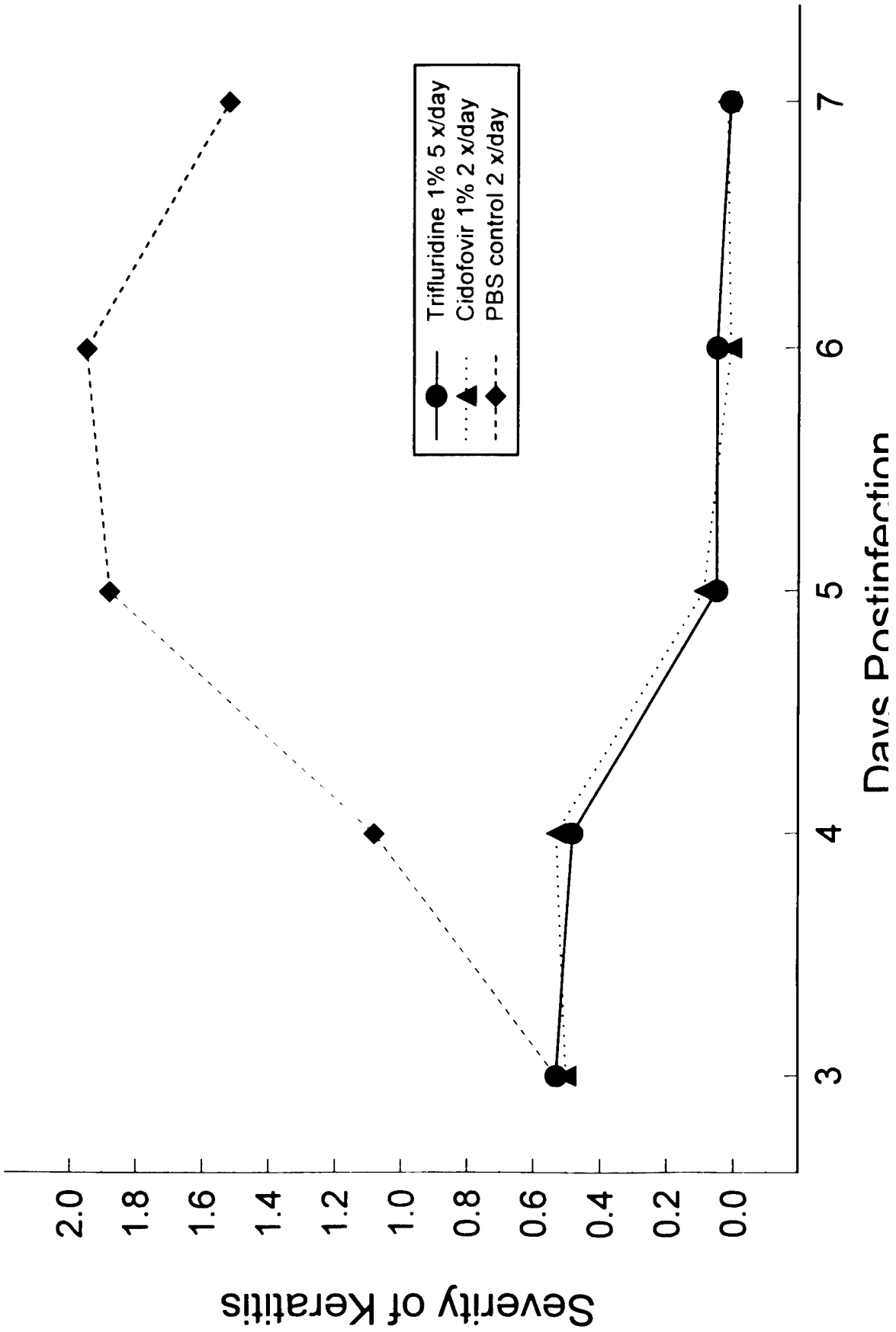

Abstract Submission Form

This form may be reproduced

A. 1. 2. 3. FOR OFFICIAL USE ONLY | 4. A10 CATEGORY (EX: 1A or G7) | 5. N P, S, O or N | 6. N/A OTHER CATEGORY

If you prefer to give an oral presentation and it cannot be accepted as such, would you present your paper as a poster? XX Yes _____ No

B. Title: The Clinical Potential Of Laser Desorption Mass Spectrometry Of Tears

C. Selected Keywords (choose no more than 4 code numbers from the list on page 6): 17 155 170 219

D. Authors, Addresses, Phone, Fax Numbers, and Internet Addresses: **(circle presenters name):**

Ray J. Varnell, Dmitri Y. Maitchouk, Victor C. Rucker, Roger W. Beuerman

LSU Eye Center
2020 Gravier Street, Suite B
New Orleans, LA 70112
504 568 6700 (Fax: 504 568 4210)

E. Signature: _____ Date: August 5, 1996

Material has not and shall not be published/presented prior to the 1997 Pittsburgh Conference.

Abstract

Provide 250 words or less in this space
Abstract may be prepared on a typewriter or laser printer and cut and pasted in this space.

The Clinical Potential Of Laser Desorption Mass Spectrometry Of Tears. Ray J. Varnell, Dmitri Y. Maitchouk, Victor C. Rucker, and Roger W. Beuerman. 2020 Gravier St, Ste B. LSU Eye Center, New Orleans, LA 70112. Telephone: 504 568 6700. Fax: 504 568 4210.

Tears provide information about several eye diseases and are easy to collect, but are available only in small quantities, as small as 1 μl or less per minute. Methods currently used to analyze tears are time-consuming and may require tears pooled from repeated collections. Matrix-assisted laser desorption/ionization mass spectrometry (MALDI) has been used to analyze single tear samples smaller than 1 μl in about 10 minutes. Tears diluted in and co-crystallized with a chemical matrix yield reproducible profiles containing 20 to 30 peaks, in which enzymes, neuropeptides, and a lipocalin were identified. Comparison of mass spectra of tears collected before and after refractive surgery revealed peaks unique to preoperative tears and other peaks unique to postoperative tears. Protocols that can be used for tear analysis have been developed for analyzing lipids, polysaccharides, and lipo- and glycoproteins. Substitutes for chemical matrices include thin films, such as polyethylene membrane or polyacrylamide gel, that are quicker and easier to use, and can be commercially produced. Improvements in instrument design are leading to quantitative analysis. Further modification of equipment and software for routine use by clinic personnel should not be difficult. (DAMD17-93-V-3013; NEI EY04074, EY02377)

Do Not Exceed This Space

Analysis of rabbit tear fluid using capillary electrophoresis with UV or laser-induced fluorescence detection

Ray J. Varnell,[a] Dmitri Y. Maitchouk,[a] Roger W. Beuerman,[a] Michael F. Salvatore,[a] James E. Carlton,[b] and Anthony M. Haag[b]

[a]*Department of Ophthalmology, Louisiana State University Medical Center School of Medicine, New Orleans, LA, U.S.A.*
[b]*Core Laboratory Facility, Louisiana State University Medical Center, New Orleans, LA, U.S.A.*

Correspondence: *Dr. Roger W. Beuerman, LSU Eye Center, 2020 Gravier St., Ste. B, New Orleans, LA 70112, U.S.A.*

Abstract

In preliminary studies of the development of tear analysis methodology that may eventually be useful in the clinical setting, the authors evaluated various protocols for analyzing rabbit tears by capillary zone electrophoresis (CZE). Conditions included the use of a 50-m*M* monosodium phosphate buffer, pH 2.5, or a 400-m*M* sodium borate buffer, pH 8.9, both with ultraviolet (UV) detection, as well as a 50-m*M* borate buffer, pH 8.5, with laser-induced fluorescence (LIF) detection of ATTO-TAG™ CBQ (Molecular Probes, Inc., Eugene, OR, U.S.A.) derivatized tears. All CZE analyses were performed with a P/ACE System 2100 instrument equipped with System Gold software (Beckman Instruments, Fullerton, CA, U.S.A.), using a 50 µm × 57 cm (50 cm to the window) fused-silica capillary, at 25 °C, with constant voltage of 20 kV for UV detection and 11 kV for LIF detection. Tear samples were collected from normal rabbit eyes by means of 10-µL glass micropipets. The volume of each sample was approximately 2 µL. Analysis using the phosphate buffer with UV detection produced as many as 35 peaks in each sample, of which 11 peaks were readily discerned. This compared favorably with sodium dodecyl sulfate-polyacrylamide gel electrophoresis (SDS-PAGE) analysis, which produced 32 bands with silver staining and 11 quantifiable bands with Coomassie brilliant blue staining. Many of the tear protein components have yet to be identified. CZE analysis with the high-ionic-strength borate buffer with UV detection produced only four peaks, and the low-ionic-strength borate buffer with LIF detection produced only six peaks. CZE analysis was completed in less than 1 hr, compared with 7–8 hr for SDS-PAGE. In summary, CZE analysis of tear fluid is comparable to CZE analysis of other bodily fluids and shows great potential for use in clinical diagnosis as well as for enhancing our understanding of the cellular actions of tears on the front of the eye.

Tear fluid has many constituents.[1,2] The nature of these constituents affects the health of the front surface of the eye,[3,4] is diagnostic for some types of ocular pathology,[5–9] and may play a role in the management of corneal wound healing.[10,11] In addition, tear collection with glass micropipets is noninvasive, inexpensive, quick, and easy. However, the volume of tears that can be collected from typical, unstimulated, normal eyes and in the case of certain diseases (e.g., dry eye syndrome) is limited to about 1 µL/min, resulting in the need to pool tear samples in previous studies. Stimulation increases tear volume by more than 50-fold,[12] but it also dramatically changes the number and variety of protein constituents in tear fluid.[13] Because of these limitations, the study of tear components has been complicated.

As noted above, studies of tear constituents have often been based on pooling of tear samples from a single donor or many donors to achieve an adequate volume of 10 µL or more of each sample type.[14,15] Relatively large sample volumes are needed if subsequent procedures involve purification and/or isolation or if the sensitivity of the analytical technique is limited.[16–18] Most of the analytical techniques used in the study of tears are time consuming, requiring many hours or days to process samples. However, with CZE, it is possible to perform a quantitative, nondestructive analysis of 2 µL of unpurified sample in less than 1 hr, with sensitivities of 10^{-9} *M* or better.[19,20]

The ultimate objective of these studies is to develop methods for analyzing human tears by CZE for clinical diagnostic purposes; however, the first phase of

Indexing terms

Tear fluid, capillary electrophoresis, laser-induced fluorescence, rabbit

Abbreviations

CZE, capillary zone electrophoresis; UV, ultraviolet; LIF, laser-induced fluorescence; SDS-PAGE, sodium dodecyl sulfate-polyacrylamide gel electrophoresis

this work has been to develop methods for experimental studies. Also, there is much information on tear composition,[21] lacrimal gland function,[22–27] corneal structure and innervation,[28–31] and corneal wound healing[32,33] already available for the rabbit model. This report describes the authors' initial work on method development for analyzing rabbit tears using CZE.

Experimental conditions and instrumentation

Tear collection and sample preparation

Tears were collected by gently pulling down the lower eyelid and collecting the liquid pooled in the lower fornix by capillary action into a fire-polished, sterile, 10-µL glass micropipet. Care was taken not to touch the surface of the eye or the soft tissue lining the inside of the eyelid to avoid stimulating reflex tears.[14] Each sample collected in this manner consisted of approximately 2 µL of tears. The sample was then either used immediately or expelled into a plastic microvial, capped, wrapped with Parafilm™ (American National Can Co., Greenwich, CT, U.S.A.), and stored at –20 °C.

Tear samples were used either undiluted or diluted. Use of undiluted tears was convenient because it was quick and simple, but there were two drawbacks. First, the volume of an undiluted tear sample was only approximately 2 µL, which would be insufficient for many CZE instruments. Second, evaporation of the aqueous phase of the tears after about an hour adversely affected the analysis, and further injections led to plugging of the column with partially solidified matter that was sometimes difficult to remove.

Diluted tear samples were expanded with distilled water without noticeably altering migration times. As expected, increasing the dilution decreased peak amplitude, but adequate sensitivity for major peaks appeared to be retained with dilutions as high as 10 volumes. Centrifugation of a diluted sample for 15 min at 1400 rpm to settle cellular material and other debris did not appear to alter the migration rates or peak detection.

CZE

For detection of tear proteins with UV light, two run buffers were used: 400 m*M* sodium borate, pH 8.9, or 50 m*M* monosodium phosphate, pH 2.5. The selection of a high-ionic-strength borate buffer was based on the observation that both serum proteins and hemoglobin variants are effectively separated by a high-ionic-strength borate buffer.[34,35] For detection with LIF, the run buffer was 50 m*M* sodium borate, pH 8.5. Samples analyzed with LIF were diluted fivefold with distilled water and mixed with ATTO-TAG CBQ reagent containing 3-(4-carboxybenzoyl)-2-quinolinecarboxaldehyde at room temperature for 30 min to form fluorescent isoindoles from the amine side groups of the tear proteins.[36]

Estimates of reproducibility were calculated from migration times of individual peaks. For samples run in phosphate buffer with UV detection, migration times were obtained for each of 11 peaks in five samples, with two to six consecutive injections of each sample. For samples run in borate buffer with UV detection, migration times were determined for each of four peaks in 10 tear samples, with two or three consecutive injections of each sample. Reproducibility was not estimated for tear samples run in borate buffer with LIF detection, because of inadequate replication. Of the eight samples analyzed under these conditions, only two had two injections each, and six samples were injected only once each.

All analyses were performed on a P/ACE System 2100, operating under System Gold software. Uncoated 50 µm × 57 cm (50 cm to the window) fused-silica capillary columns were used at 25 °C. A constant voltage of 20 kV was used with UV detection and 11 kV with LIF detection. UV detection used the 214-nm wavelength, and LIF detection used an argon ion laser excitation beam with a 488-nm wavelength, with detection of light at 520 nm.

Before each run, the column was prerinsed with 0.1 N sodium hydroxide regenerator solution (Beckman Instruments) for 2 min, followed by distilled water for 4 min. Next, the column was pretreated with run buffer for 2 min, followed by hydrostatic injection of sample contained in polyolefin microvials (Beckman Instruments) for 8 sec to introduce approximately 12 nL into the column.

SDS-PAGE

Rabbit tears were analyzed by SDS-PAGE for comparison with the CZE results. Tears from normal rabbit eyes were collected as described above, centrifuged briefly, and stored at –80 °C. For analysis, a tear sample was thawed and diluted with 50 µL of 1% SDS and 25 µL of 3× reducing sample buffer, supplemented with dithiothreitol, and applied to a 14.5% acrylamide gel. The gel retained rabbit tear proteins ranging in molecular weight from approximately 6 to 150 kD, while optimizing their separation. After electrophoretic separation was complete, silver staining was used to detect the maximum number of protein bands, and Coomassie brilliant blue was used for qualitative protein determination. Expendable supplies for SDS-PAGE analysis were obtained from Fisher Scientific (Pittsburgh, PA, U.S.A.) and Bio-Rad (Hercules, CA, U.S.A.).

Densitometric scanning of cellophane-sealed and dried gels was done with a Microtek (Redondo Beach, CA, U.S.A.) ScanMaker IIHR flatbed scanner, in grayscale, with 720-dpi resolution, and equipped with

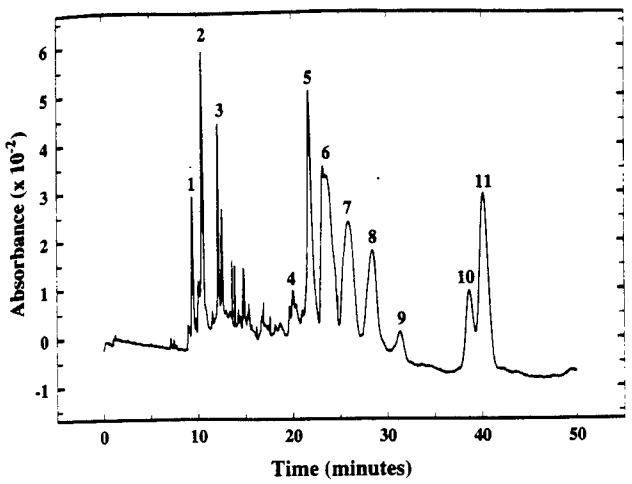

FIGURE 1 *CZE electropherogram of rabbit tears performed using 50 mM phosphate running buffer, pH 2.5, at 20 kV and 23 °C, with UV detection at 214 nm. At least 35 peaks are seen in this profile. Relative migration rates were determined for the peaks numbered 1 through 11 (see* Table 1*).*

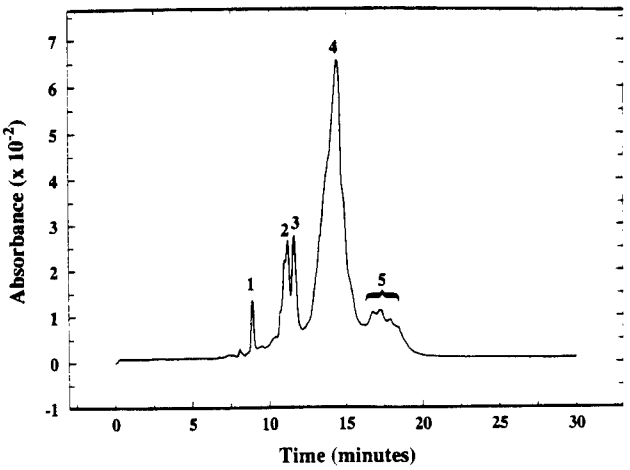

FIGURE 2 *CZE electropherogram of rabbit tears performed using 400 mM borate running buffer, pH 8.9, at 20 kV and 23 °C, with UV detection at 214 nm.*

Table 1
MIGRATION CHARACTERISTICS FOR 11 PEAKS OBSERVED IN ELECTROPHEROGRAMS OF RABBIT TEARS RUN IN 50 mM MONOSODIUM PHOSPHATE BUFFER, pH 2.5, AT 20 kV AND 23 °C

	Peaks										
Statistics*	1	2	3	4	5	6	7	8	9	10	11
Mean	8.6	9.5	10.7	18.0	19.1	20.2	21.9	23.8	25.6	35.6	35.3
SD	0.8	0.9	1.3	2.0	2.5	3.1	3.7	4.2	4.7	5.0	5.2
%RSD	1.7	2.1	1.7	2.3	2.4	3.2	3.4	3.5	3.7	5.2	4.7

*Mean, average migration time for N = five samples with two to six injections each; SD, standard deviation; %RSD, relative migration rate.

Adobe Photoshop™ 3.0 (Adobe Systems, Inc., Seattle, WA, U.S.A.) and ScanMaker Plug-In 2.13 software. Saved images were analyzed in accordance with Chow and Evans[37] using NIH Image 1.60 software (National Institutes of Health, Bethesda, MD, U.S.A.). To determine the relative amount of protein in each band, the area under the peak for each band was divided by the integral value of the entire scanned lane, and the quotient was converted to percent total protein.

Results

CZE with 50 mM phosphate buffer and UV detection

The CZE analysis of rabbit tears with 50 m*M* phosphate buffer at pH 2.5 resulted in good resolution of a large number of peaks. At least 35 peaks can be seen in the representative electropherogram shown in *Figure 1*. Of the peaks detected with this buffer, 11 could be distinguished in each of five samples analyzed. Average migration time, standard deviation, and relative migration rate for each of the 11 peaks are shown in Table 1. Although examination of average migration times and standard deviations indicates that the migration times for several of the peaks may overlap and that, on average, peak 11 might appear before peak 10, these indications are artifacts due to sampling, arising primarily because no attempt was made to account for differences in electroosmotic flow. Run time with this buffer, at 20 kV, was 45–50 min.

Peak 11 was collected electrostatically from four consecutive injections and contained a single protein, according to subsequent analysis by laser desorption, time-of-flight mass spectrometry. Trypsin digest of the protein produced 16 fragments, two of which, when compared with entries in the OWL.r27.1 database (RW Nelson, Department of Chemistry and Biochemistry, Arizona State University, Tempe, AZ, U.S.A.; personal communication), appeared to match with mouse cryptdins, members of the family of mammalian defensins involved in immunity to infection and neoplasia. However, this rate of matching was considered inadequate, and the identity of this protein remains uncertain.

CZE with 400 mM borate buffer and UV detection

The 400-m*M* borate buffer at pH 8.9 with UV detection yielded a distinctive electropherogram of rabbit tears (*Figure 2*), consisting of four well-defined peaks and a mass of poorly resolved material. On average, at 20 kV and 75–80 µamps of current, peaks 1, 2, 3, and 4 appeared at approximately 8.3 ± 0.6, 10.2 ± 1.0, 10.5 ± 1.1, and 12.6 ± 1.3 min (mean ± standard deviation), respectively. Relative migration rates, without controlling for differences in electroosmotic flow, were 5.3%, 7.0%,

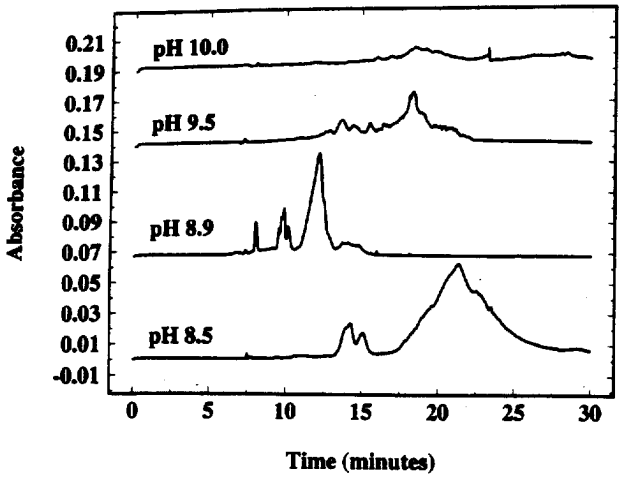

FIGURE 3 *CZE electropherograms of rabbit tears performed using 400 mM borate running buffer, at various pHs, at 20 kV and 23 °C, with UV detection at 214 nm.*

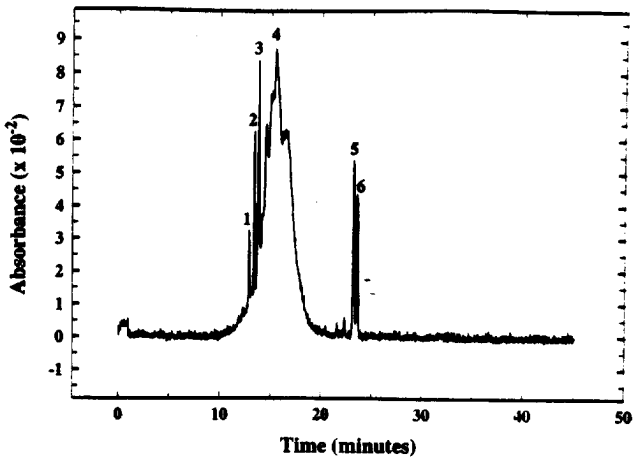

FIGURE 4 *CZE electropherogram of rabbit tear protein derivatized with ATTO-TAG CBQ, performed using 50 mM borate running buffer, pH 8.5, at 11 kV and 23 °C, with LIF detection.*

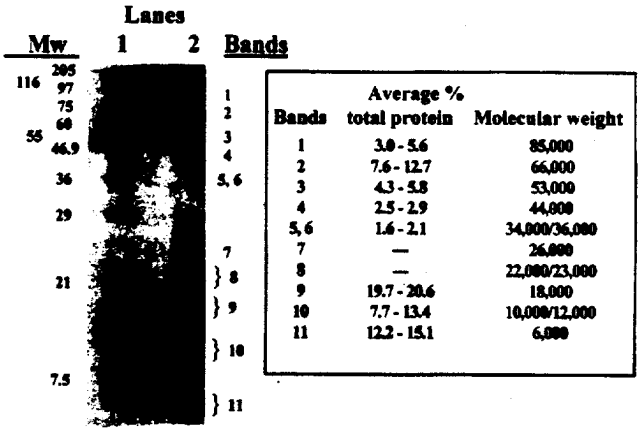

Bands	Average % total protein	Molecular weight
1	3.0 - 5.6	85,000
2	7.6 - 12.7	66,000
3	4.3 - 5.8	53,000
4	2.5 - 2.9	44,000
5, 6	1.6 - 2.1	34,000/36,000
7	—	26,000
8	—	22,000/23,000
9	19.7 - 20.6	18,000
10	7.7 - 13.4	10,000/12,000
11	12.2 - 15.1	6,000

FIGURE 5 *A 14.5% SDS-PAGE gel of molecular weight standards from about 6 kD to 116 kD (lane 1) and rabbit tear proteins (lane 2). Numbered bands in lane 2 correspond to band numbers in the table. Stained with Coomassie brilliant blue.*

6.7%, and 8.7%, respectively. In some samples, a few small peaks appeared at approximately 6–7 min (Figure 2), and others appeared after 20 min. Although variations in peak size, shape, and migration rate were apparent among samples, the basic pattern of peaks, as illustrated in Figure 2, was maintained. Separations with this buffer were complete in 25–30 min.

Use of the borate buffer at other pHs ranging from 7.0 to 10.5 resulted in poorer resolution and/or separation of peaks, as illustrated in *Figure 3* for pHs 8.5, 8.9, 9.5, and 10.0. Also with this buffer, lower voltage resulted in longer separation times and higher risk of sample degradation after the second injection, whereas voltages higher than 20 kV raised the current load over 100 µamps, increasing the risk of joule heating and denaturation of the sample within the column.

CZE with 50 mM borate buffer and LIF detection

Analysis of derivatized rabbit tear proteins using a 50-m*M* borate buffer at pH 8.5 with LIF detection resulted in electropherograms with six principal peaks (*Figure 4*). Separations obtained with this buffer and LIF detection were comparable to separations obtained with the high-ionic-strength borate buffer at about the same pH with UV detection, although the LIF detection protocol produced two additional peaks and a different peak profile. No attempt was made to determine migration times, standard deviations, and relative rate of migration of peaks obtained by LIF detection because, of the eight samples analyzed, only two were injected more than once.

SDS-PAGE

Examination of silver-stained gel slabs indicated 32 protein bands from undiluted, pooled tears of normal rabbit eyes. Of these 32 bands, 11 were quantifiable when gels were stained with Coomassie brilliant blue (*Figure 5*). Sample preparation, electrophoresis, postseparation staining, drying of the gel, and densitometric scanning required about 7–8 hr with the use of commercially prepared gels. Two more hours would have been required if the gel slabs had been prepared in the laboratory. Software analysis of the scanning data to obtain the percent total protein and estimated molecular weights (Figure 5) required an additional 2 hr. In fact, the requirement for about 10 µL of undiluted tears per lane provided only one analytical run.

Discussion

Of the three methods developed for the CZE analysis of rabbit tears, the method involving the 50-m*M* phosphate buffer, pH 2.5, with UV detection provided the best separations. The detection of about 35 peaks in rabbit tears by CZE compared favorably with the 32 bands detected by silver-stained SDS-PAGE. Interestingly, 11 peaks from CZE and 11 bands from SDS-PAGE were analyzable. However, whether the proteins represented by the 11 CZE peaks correspond in any way to the proteins represented by the 11 SDS-PAGE bands is not yet known. Another similarity between these analytical methods is that intact, native proteins can be recovered for further study from both CZE and SDS-PAGE, although this can be accomplished perhaps somewhat more easily and efficiently, in less time, with automated fraction collection in CZE. Further detection of included proteins in a collected fraction can be analyzed rapidly using time-of-flight mass spectrometry.

Run time with the phosphate buffer was slightly longer than that with either of the borate buffers, but run time for each of the three methods was less than 1 hr, including preparation time for samples analyzed with LIF detection. Clearly, CZE run times of less than 1 hr are an improvement over the 7–8 hr needed to acquire densitometric scans for comparable samples run on SDS-PAGE. CZE runs times of tears might be reduced to less than 30 min by using smaller diameter columns.[34]

Guzman et al.[38] included human tears in their discussion of the use of CZE of body fluids in clinical diagnosis. Chen et al.[39] used CE/LIF to determine glucose levels in human tears as a possible noninvasive way to monitor serum levels of glucose in diabetes mellitus. The present authors' methods for the analysis of tear fluid with phosphate buffer at pH 2.5 are comparable to those for CZE analyses of urine[40,41] and saliva,[42,43] in that all of these body fluids can be obtained by noninvasive methods and samples can be used undiluted and unpurified. Furthermore, run times are 1 hr or less. In other diagnostic situations, methodology may be more problematic. Whether undiluted, unpurified sweat, which also can be collected noninvasively and in which electrolyte concentrations are diagnostic for cystic fibrosis,[5] can be successfully analyzed by CZE seems to be undetermined. Other bodily fluids, such as blood, cerebrospinal fluid, bile, and kidney dialysate, involve nontrivial invasive methods for sample collection, and blood samples must be separated into at least serum or plasma before analysis with CZE.

The fact that CZE separations of rabbit tear proteins with either low- or high-ionic-strength borate buffers at moderately high pH yielded only a few well-defined peaks (Figures 2 and 5) suggests two correlated conclusions. First, each of these peaks probably represents multiple, comigrating proteins. Second, routine profiling of tears by CZE under these conditions is not feasible, since it does not provide resolution of the constituents. Although UV detection and either buffer would allow individual peaks to be collected and further analyzed, further utilization of tear proteins following LIF detection is severely restricted, owing primarily to the fact that the derivatized proteins cannot be readily converted back to their original state. Thus, analysis of tears under conditions for LIF detection may be useful primarily for detecting substances that are present at very low concentrations in tears.

Conclusion

A method was developed for rapid, easy, and reasonably informative analysis of rabbit tears, using CZE with UV detection and phosphate buffer at pH 2.5. The development of this method will allow us to identify individual constituents of rabbit tears and to investigate the effects of these constituents on ocular wounding.

Tears are the extracellular fluid that bathes the front of the eye and contains growth-stimulating and regulatory proteins. Studies begun in the authors' laboratory have shown that variations in tear constituents are observed from individual to individual and may be associated with specific ocular conditions. As reported here, rapid, accurate analysis of small volumes of tear fluid is feasible. Extending this study to specific conditions, such as inflammation, could make tear analysis practical on a clinical basis.

Acknowledgments

These studies were supported in part by U.S. Public Health Service grants EY04074 and EY02377 (Core grant) from the National Eye Institute, National Institutes of Health, Bethesda, MD, U.S.A., as well as the Department of the Army, Cooperative Agreement DAMD17-93-V-3013. (This does not necessarily reflect the position or the policy of the Government, and no official endorsement should be inferred.)

Manuscript received December 20, 1996.

References

1. van Haeringen NJ. Clinical biochemistry of tears. Surv Ophthalmol 1981; 26:84–96.
2. Farris RL. Abnormalities of the tears and treatment of the eyes. In: Kaufman HE, Barron BA, McDonald MB, Waltman SR, eds. The cornea. New York: Churchill Livingstone, 1988: 539–557.
3. Kessing AV. A new division of the conjunctiva on the basis of X-ray examination. Acta Ophthalmol 1967; 45:680–8.

4. Stern ME, Beuerman RW, Fox RL, Gao J, Mircheff AK, Pflugfelder SC. A unified theory of the role of the ocular surface in dry eye. Adv Exp Med Biol 1997; in press.
5. Haeckel R, Hänecke P. The application of saliva, sweat and tear fluid for diagnostic purposes. Ann Biol Clin 1993; 50:903–10.
6. Mackie IA, Seal DV. Diagnostic implications of tear protein profiles. Br J Ophthalmol 1984; 68:321–4.
7. Danjo Y, Lee M, Horimoto K, Hamano T. Ocular surface damage and tear lactoferrin in dry eye syndrome. Acta Ophthalmol 1994; 72:433–7.
8. Comerie-Smith SE, Nunez J, Hosmer M, Farris RL. Tear lactoferrin levels and ocular bacterial flora in HIV positive patients. Adv Exp Med Biol 1994; 350:339–44.
9. Cheng KH, Spanjaard L, Rutten H, Dankert J, Polak BCP, Kijlstra A. Immunoglobulin A antibodies against *Pseudomonas aeruginosa* in the tear fluid of contact lens wearers. Invest Ophthalmol Vis Sci 1996; 37:2081–8.
10. Naqui R, Ji Z, Pflugfelder SC. Immune cytokine RNA expression by human conjunctival epithelium after superficial microtrauma. ARVO abstract. Invest Ophthalmol Vis Sci 1996; 37(suppl):S356.
11. Beuerman RW, Maitchouk DY, Varnell RJ, Pedroza-Schmidt L. Interactions between lacrimal function and the ocular surface. In: Kinoshita S, Ohashi Y, eds. Proceedings of the 2nd Kyoto Cornea Club. PMSI Japan: Tokyo. 1997; in press.
12. Fullard RJ, Snyder C. Protein levels in nonstimulated and stimulated tears of normal human subjects. Invest Ophthalmol Vis Sci 1990; 31:1119–26.
13. Fullard RJ, Tucker D. Tear protein composition and the effects of stimulus. Adv Exp Med Biol 1994; 350:309–14.
14. Fullard RJ, Tucker DL. Changes in human tear protein levels with progressively increasing stimulus. Invest Ophthalmol Vis Sci 1991; 32:2290–301.
15. Kuizenga A, van Haeringen NJ, Kijlstra A. Identification of lectin binding proteins in human tears. Invest Ophthalmol Vis Sci 1991; 32:3277–84.
16. Varnell RJ, Yan-Freeman J, Maitchouk D, Beuerman RW, Gebhardt BM. Detection of substance P in human tears by laser desorption mass spectrometry and immunoassay. Curr Eye Res 1997; in press.
17. Fukuda M, Fullard RJ, Willcox MDP, et al. Fibronectin in the tear film. Invest Ophthalmol Vis Sci 1996; 37:459–67.
18. Meijer F, van Haeringen NJ. Separation and characteristics of glycoproteins in tears which inhibit coating and precipitation of protein. Curr Eye Res 1993; 12:531–8.
19. Cheng YF, Dovichi NJ. Subattomole amino acid analysis by capillary zone electrophoresis and laser-induced fluorescence. Science 1988; 242:562–4.
20. Burolla VP, Pentoney SL Jr, Zare R. High performance capillary electrophoresis. Am Biol Lab 1989; Nov/Dec:20–6.
21. Varnell RJ, Maitchouk DY, Beuerman RW, Carlton JE, Haag A. Small-volume analysis of rabbit tears and effects of a corneal wound on tear protein spectra. Adv Exp Med Biol 1997; in press.
22. Dartt DA, Knox I, Palau A, Botelho SY. Proteins in fluids from individual orbital glands and in tears. Invest Ophthalmol Vis Sci 1980; 19:1342–7.
23. Bromberg B. Autonomic control of lacrimal protein secretion. Invest Ophthalmol Vis Sci 1981; 20:110–6.
24. Dartt DA. Signal transduction and control of lacrimal gland protein secretion: a review. Curr Eye Res 1989; 8:619–36.
25. Shirolka S, Schoenqald RD, Barfknecht CF, et al. Lacrimal secretion stimulants: sigma receptors and drug implications. J Ocul Pharmacol 1993; 9:211–27.
26. Chesnokova NB, Kuznetsova TP, Sosulina NE. Study of the lacrimal fluid proteolytic enzymes and their inhibitors in inflammatory diseases of the cornea. Vestn Oftalmol 1994; 110:20–2.
27. Gierow JP, Lambert RW, Mircheff AK. Fluid phase endocytosis by isolated rabbit lacrimal gland acinar cells. Exp Eye Res 1995; 60:511–25.
28. Beuerman RW, Schimmelpfennig B. Sensory denervation of the rabbit cornea affects epithelium properties. Exp Neurol 1980; 69:196–201.
29. Rozsa A, Beuerman RW. Density and organization of free nerve ending of rabbit corneal epithelium. Pain 1982; 14:105–20.
30. Klyce SD, Jenison GL, Crosson CE, Beuerman RW. Distribution of sympathetic nerves in the rabbit cornea. ARVO abstract. Invest Ophthalmol Vis Sci 1986; 27(suppl):354.
31. Beuerman RW, Tanelian DL, Schimmelpfennig B. Nerve tissue interactions in the cornea. In: Cavanagh D, ed. The cornea: transactions of the world congress on the cornea III. New York: Raven Press, 1988:59–62.
32. Reidy JJ, Zarzour J, Thompson HW, Beuerman RW. Effect of topical beta blockers on corneal wound healing in the rabbit. Br J Ophthalmol 1994; 78:377–80.
33. Thompson HW, Beuerman RW, Cook J, Underwood LW, Nguyen DH. Transcription of message for tumor necrosis factor-α by lacrimal gland is regulated by corneal wounding. Adv Exp Med Biol 1994; 350:211–7.
34. Chen F-TA, Kelly L, Palmieri R, Biehler R, Schwartz H. Use of high ionic strength buffers for the separation of proteins and peptides with capillary electrophoresis. J Liq Chromatogr 1992; 15:1143–61.
35. Chen F-TA. High-resolution protein analysis by automated capillary electrophoresis. Clin Chem 1992; 38:1651–3.
36. Liu J, Hsieh Y-Z, Wiesler D, Novotny M. Design of 3-(4-carboxybenzoyl)-2-quinolinecarboxaldehyde as a reagent for ultrasensitive determination of primary amines by capillary electrophoresis using laser fluorescence detection. Anal Chem 1991; 63:408–12.
37. Chow D, Evans J. NIH Image 1.60 tutorial. Using Image for densitometric analysis of 1-D gels. National Institutes of Health. Available electronically from http://scrc.dcrt.nih.gov/imgproc/nihimage/gel_density/table.html.
38. Guzman NA, Gonzalez CL, Trebilcock MA, Lernandez L, Berck CM, Advis JP. The use of capillary electrophoresis in clinical diagnosis. In: Guzman NA, ed. Capillary electrophoresis technology. New York: Marcel Dekker, 1993:643–72.
39. Chen R, Jin Z, Colón LA. Analysis of tear fluid by CE/LIF: a noninvasive approach for glucose monitoring. J Cap Elec 1996; 3(5):243–8.
40. Jellum E. Capillary electrophoresis for medical diagnosis. J Cap Elec 1994; 1:97–105.
41. Chen F-TA, Liu C-M, Hsieh Y-Z, Sternberg JC. Capillary electrophoresis—a new clinical tool. Clin Chem 1991; 37:14–9.
42. Rodopoulos N, Hojvall L, Norman A. Elimination of theobromine metabolites in healthy adults. Scand J Clin Lab Invest 1996; 56:373–83.
43. Perrett D, Ross GA. Rapid determination of drugs in biofluids by capillary electrophoresis. Measurement of antipyrine in saliva for pharmacokinetic studies. J Chromatogr A 1995; 700:179–86.

SHORT COMMUNICATION

Detection of substance P in human tears by laser desorption mass spectrometry and immunoassay

Ray J. Varnell, Jiong Yan Freeman, Dmitri Maitchouk, Roger W. Beuerman and Bryan M. Gebhardt

LSU Eye Center, Louisiana State University Medical Center, School of Medicine, New Orleans, LA, USA

Abstract

Purpose. To determine whether substance P is present in human tears.

Methods. Tear samples (1–2 μl) were collected from one eye of each of 12 subjects. Two of the eyes had dry eye syndrome, two wore contact lenses and had dry eye syndrome, and eight were normal. Five of the eight normal eyes were scheduled to undergo excimer laser refractive surgery, and tears were collected from these eyes before and after surgery. Tear samples were analyzed by laser desorption mass spectrometry. Pooled samples from one individual were subjected to enzyme-linked immunoabsorbent assay.

Results. Laser desorption mass spectra of the 18 tear samples displayed well defined peaks with mass to charge (m/z) ratios ranging from 1343.7 to 1355.9 and/or 1356.9 to 1364.7, corresponding to an average m/z of 1349.8 ± 1.13 for protonated substance P and 1361.2 ± 0.54 for oxidized substance P obtained from 14 mass spectra of standards formulated with substance P concentrations ranging from 10^{-4} M to 10^{-12} M. As confirmation, an enzyme-linked immunoabsorbent assay performed twice on pooled tears from one eye detected substance P in both replicates at a concentration of 125 pg/ml (9.26×10^{-11} M).

Conclusions. These findings demonstrate that substance P is a component of tears obtained from normal eyes of men and women ranging in age from 26 to 60 years, from eyes fitted with contact lenses, from eyes with dry eye syndrome, and from eyes 1 and 2 days after excimer laser refractive surgery. Whether the concentration of substance P in tears varies with sex, age, or eye condition, the source of substance P in tears, and its role in tears remains to be discovered. Curr. Eye Res. 16: 960–963, 1997.

Key words: human tears, immunoassay, laser desorption mass spectrometry, substance P

Substance P is a neuropeptide that promotes secretion by exocrine glands (1) and may act as a neurotransmitter or modulator in the central and peripheral nervous system (2). A substance P-like material is present in homogenates of the choroid, retina, optic nerve, optic nerve head, uvea, iris sphincter region, iris dilator and ciliary body, conjunctiva, whole upper eyelid, lacrimal gland, Harderian gland, and extraorbital muscle of the rabbit eye (3, 4, 5). In the densely innervated cornea (6), sensory fibers are positive for substance P (3). Substance P normally is not present or is present only in very low amounts in the aqueous humor of rabbits (5), but a peptide with substance P-like immunoreactivity is released into the aqueous humor when the trigeminal nerve is stimulated (7).

In lacrimal gland sections from rats, guinea pigs, and monkeys, nerve fibers that are immunohistochemically positive for substance P or substance P-like material are located around blood vessels and ducts (8, 9). Based on these findings, Nikkinen *et al.* (9) and Matsumoto *et al.* (8) suggested that substance P may be an important modulator of lacrimal gland secretion. In support of this, Williams *et al.* (10) demonstrated that the number of nerves staining positively for substance P or substance P-like material in rat lacrimal glands declines as the animal ages, and suggested that the decline in substance P-containing nerves corresponds with and may be a contributing factor to reduced tear output in older animals. Another possible role of substance P may be in promoting cellular growth (11, 12) and the production of extracellular matrix (11).

Substance P has recently been detected in human nasal lavage fluid (13). Because lacrimal secretions contribute to

Correspondence: Dr. Roger W. Beuerman, LSU Eye Center, 2020 Gravier Street, Suite B, New Orleans, LA 70112, USA

This work was presented in part as a paper at the annual meeting of the Association for Research in Vision and Ophthalmology, Fort Lauderdale, Florida, April 21, 1996.

Received on January 28, 1997; revised and accepted on April 30, 1997

nasal fluids via the tear drainage system, it is reasonable to suspect that substance P also occurs in tears.

In this study, we used matrix-assisted desorption/ionization mass spectrometry (MALDI) and the enzyme-linked immunoabsorbant assay (ELISA) to determine whether substance P can be detected in human tears. MALDI was employed because it is sensitive to the low femtomole range, requires less than a microliter of sample, and is tolerant of salts and other impurities in the complex mixtures typical of body fluids (14). ELISA was used to confirm the MALDI results.

Unstimulated tears (approximately 1 μl/min) were collected from the inferior cul-de-sac with fire-polished 10-μl micropipettes. After collection, tears were either used immediately or stored in capped, 400-μl, polyethylene microcentrifuge tubes at –20°C. Tears were collected from one eye of each of 12 healthy subjects. Subject age ranged from 26 to 60 years. Six subjects were men and six were women. Eight subjects had normal eyes, i.e. were disease-free and did not wear contact lenses; four subjects had been diagnosed with dry eye syndrome. Dry eyes were associated with wearing contact lenses for two subjects, with rheumatoid arthritis for one subject, and with an unknown etiology in another subject, although the latter subject had mild anterior blepharitis, possible insufficient night-time lid closure, and a familial history of arthritis and lupus. Five of the eight subjects with normal eyes were excimer laser photorefractive keratectomy (PRK) patients, and their tears were collected before surgery and on the first and/or second day after PRK. Seven postoperative samples were collected, but one preoperative sample was lost. Thus, a total of 18 tear samples were analyzed.

For MALDI, each tear sample was mixed 1:100, v:v, with matrix. The matrix was freshly prepared daily by dissolving an excess of α-cyano-4-hydroxycinnamic acid (Aldrich Chemical Co., Milwaukee, WI) in HPLC-grade acetonitrile containing 0.1% trifluoroacetic acid and diluting the resulting solution 1:1, v:v, with an aqueous solution of 0.1% trifluoroacetic acid. A 0.5 μl aliquot of tear-matrix solution was spotted on a stainless steel plate and allowed to air-dry for a few min until crystals of matrix and embedded protein formed (15). The plate was then introduced into a linear MALDI time-of-flight mass spectrometer (Voyager™ Biospectrometry™ Workstation, PerSeptive Biosystems, Framingham, MA) for analysis. The final mass spectrum generated from the analysis of each sample was averaged over 256 individual single-pulse spectra.

To prepare the standard solutions, substance P was obtained commercially (Cat # S 6883, Sigma Chemical Co. St. Louis, MO) and reconstituted in physiologically balanced, unpreserved sterile salt solution (Alcon Laboratories, Inc., Fort Worth, TX) at concentrations ranging from 10^{-4} to 10^{-12} M (1.35 picograms/ml). Balanced salt solution containing sodium, potassium, calcium, and magnesium salts was used, because it is similar to the aqueous phase of tears. Aliquots of the standard substance P solutions were mixed with the α-cyano-4-hydroxycinnamic acid matrix and processed for mass spectrometry in the same manner as the tear samples.

To construct the mass spectra for the tear samples and substance P standards, the ratio of mass to charge (m/z) was plotted on the abscissa and signal intensity in arbitrary units was plotted on the ordinate (Figs. 1 and 2). Figure 1 is a spectrum of a human tear sample. In Figure 2 (top), a part of the spectrum from Figure 1 was enlarged to show substance P at m/z = 1351 and oxidized substance P at m/z = 1366; for comparison, spectra of a subsample of the tears from Figure 1 with substance P added (Fig. 2, middle) and a substance P standard (Fig. 2, bottom) were included. All of the 18 tear samples analyzed with MALDI showed a well-defined peak in the m/z range from 1343.7 to 1355.9 or from 1356.9 to 1364.7. These results corresponded to an average m/z of 1349.8 ± 1.13 for

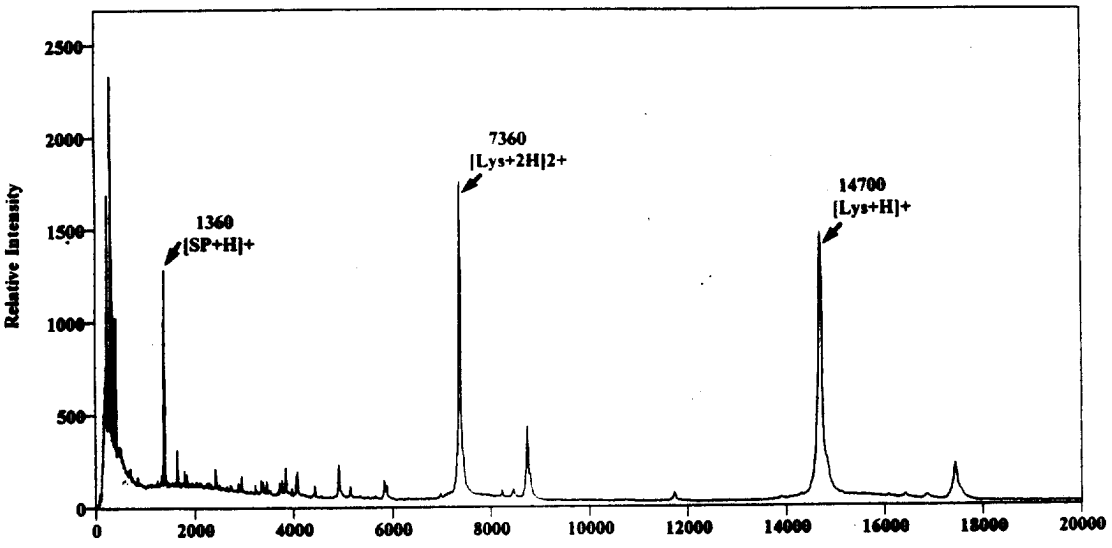

Figure 1. A MALDI mass spectrum of substance P (m/z = 1360) naturally occurring in undiluted tears collected from a healthy 28-year-old man who did not wear contact lenses and who was asymptomatic for dry eye syndrome. Lys+H and Lys+2H are lysozyme and its doubly protonated form, respectively (2).

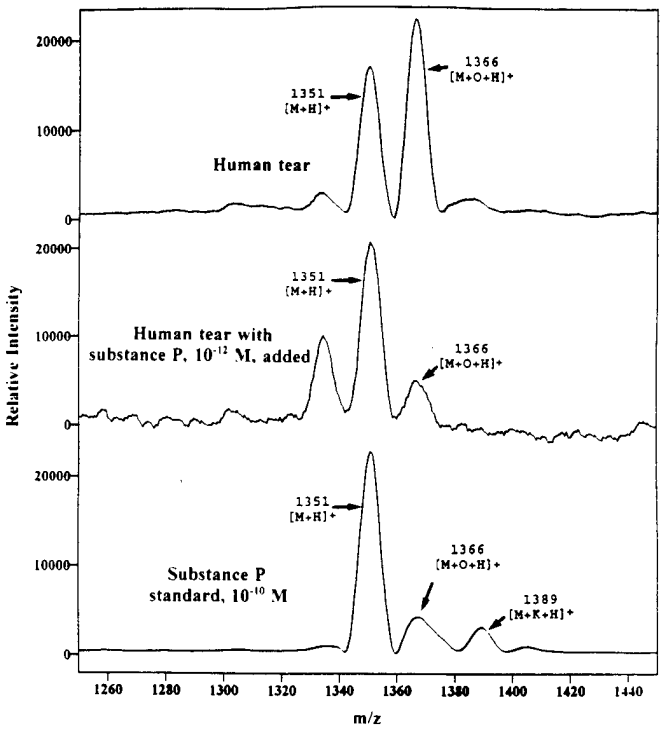

Figure 2. Top: The mass spectrum of substance P (m/z = 1351) in human tears from Figure 1. Middle: Tears from the same subject with substance P added at a concentration of 10^{-12} M. Bottom: Substance P standard at a concentration of 10^{-10} M in saline solution. In each tracing, the peak at m/z = 1366 is oxidized substance P. In the bottom tracing, the peak at m/z = 1389 is the potassium adduct of substance P; the potassium is provided by the saline solution.

protonated substance P $[M + H]^+$ and 1361.2 ± 0.54 for oxidized substance P $[M + O + H]^+$ obtained from the 14 mass spectra of substance P standards with concentrations ranging from 10^{-1} M to 10^{-12} M.

A few other peaks in Figures 1 and 2 were tentatively identified. In Figure 1, peaks with m/z = 14,700 and m/z = 7360 appeared to be the singly protonated and doubly protonated ions of lysozyme, because they coincided with these peaks in the mass spectrum of the enzyme, as previously reported (16). In the mass spectrum of the substance P standard (Fig. 2, bottom), the low intensity peak at m/z = 1389 probably was the potassium adduct of substance P, which was contributed by the balanced salt solution. The difference in the m/z between the peak for substance P and the peak for the adduct was 38 mass units, which was within experimental error for the measurement of potassium at 39 mass units. When the standard solution was added to tears (Fig. 2, middle), the potassium-adduct peak was absent from the spectrum and presumably was suppressed. Other peaks in Figures 1 and 2 were unidentified.

An Enzyme Immunoassay Kit (Cat # 583751, Cayman Chemical, Ann Arbor, MI) for substance P was used for ELISA analysis of tears. Tears from one eye of one subject (a woman) were collected and frozen at –20°C until 100 μl had been obtained, then pooled and divided equally into two wells of the test plate, in accordance with the manufacturer's directions. The analysis was performed in duplicate. Substance P was detected in both replicates. The concentration of substance P in the tears from this subject was 125 pg/ml (9.26×10^{-11} M).

These findings demonstrate that substance P is a component of the tears obtained from normal eyes of men and women ranging in age from 26 to 60 years, from eyes fitted with contact lenses, from eyes with dry eye syndrome, and from eyes 1 and 2 days after excimer laser refractive surgery. However, we have not yet determined whether the concentration of substance P in tears varies with sex, age, or eye condition, and the source of substance P and its role in tears remain to be discovered.

Acknowledgments

This study was supported in part by EY04074 (RWB) and EY02377 (CORE grant; LSU Eye Center) from the National Eye Institute, National Institutes of Health, Bethesda, MD; Department of the Army, Cooperative Agreement DAMD17-93-V-3013 (This does not necessarily reflect the position or the policy of the government, and no official endorsement should be inferred.); and an unrestricted departmental grant from Research to Prevent Blindness, Inc., New York.

References

1. Rudich, L. and Butcher, F. R. (1976) Effects of substance P and eledoisin on K efflux, amylase release and cyclic nucleotide levels in slices of rat parotid gland. *Biochim. Biophys. Acta*, **444,** 704–711.
2. Hökfelt, T., Johansson, O., Ljungdahl, Å., Lundberg, J. M. and Schultzberg, M. (1980) Peptidergic neurones. *Nature*, **284,** 515–521.
3. Butler, J. M., Powell, D. and Unger, W. G. (1980) Substance P levels in normal and sensorially denervated rabbit eyes. *Exp. Eye Res.* **30,** 311–313.
4. Butler, J. M., Ruskell, G. L., Cole, D. F., Unger, W. G., Zhang, S. Q., Blank, M. A., McGregor, G. P. and Bloom, S. R. (1984) Effect of VIIth (facial) nerve degeneration on vasoactive intestinal polypeptide and substance P levels in ocular and orbital tissues of the rabbit. *Exp. Eye Res.* **39,** 523–532.
5. Unger, W. G., Butler, J. M., Cole, D. F., Bloom, S. R. and McGregor, G. P. (1981) Substance P, vasoactive intestinal polypeptide (VIP) and somatostatin levels in ocular tissue of normal and sensorially denervated rabbit eyes (Letter). *Exp. Eye Res.* **32,** 797–801.
6. Rozsa, A. and Beuerman, R. W. (1982) Density and organization of free nerve endings of rabbit corneal epithelium. *Pain*, **14,** 105–120.
7. Bill, A., Stjernschantz, J., Mandahl, A., Brodin, E. and Nilsson, G. (1979) Substance P: release on trigeminal nerve stimulation, effects in the eye. *Acta Physiol. Scand.* **106,** 371–373.
8. Matsumoto, Y., Tanabe, T., Ueda, S. and Kawata, M. (1992) Immunohistochemical and enzymehistochemical

studies of peptidergic, aminergic and cholinergic innervation of the lacrimal gland of the monkey (*Macaca fascata*). *J. Auton. Nerv. Syst.* **37,** 207–214.

9. Nikkinen, A., Lehtosalo, J. I., Uusitalo, H., Palkama, A. and Panula, P. (1984) The lacrimal glands of the rat and the guinea pig are innervated by nerve fibers containing immunoreactivities for substance P and vasoactive intestinal polypeptide. *Histochemistry*, **81,** 23–27.
10. Williams, R. M., Singh, J. and Sharkey, K. A. (1994) Innervation and mast cells of the rat exorbital lacrimal gland: the effects of age. *J. Auton. Nerv. Syst.* **47,** 95–108.
11. Reid, T. W., Murphy, C. J., Iwahashi, C. K., Fontes, B. A. and Mannis, M. J. (1993) Stimulation of epithelial cell growth by the neuropeptide substance P. *J. Cell. Biochem* **52,** 476–485.
12. Reid, T., Nilsson, J., von Euler, A. M. and Dalsgaard, C.-J. (1985) Stimulation of connective tissue cell growth by substance P and substance K. *Nature*, **315,** 61–63.
13. Schultz, K.-D., Furkert, J., O'Conner, A., Böttcher, M., Schmidt, M., Baumgarten, C. R. and Kunkel, G. (1996) Determination of substance P in human nasal lavage fluid. *Neuropeptides*, **30,** 117–124.
14. Hillenkamp, F., Karas, M., Beavis, R. C. and Chait, B. T. (1991) Matrix-assisted laser desorption/ionization mass spectrometry of biopolymers. *Anal. Chem* **63,** 1193A–1203A.
15. Beavis, R. C., Chaudhary, T. and Chait, B. T. (1992) α-Cyano-4-hydroxycinnamic acid as a matrix for matrix-assisted laser desorption mass spectrometry. (Letter). *Organic Mass Spectrom.* **27,** 156–158.
16. Maitchouk, D. Y., Varnell, R. J., Beuerman, R. W., Yan, J. (1996) Analyzing proteins in tears from patients with dry eye syndrome, with contact lenses, or undergoing photorefractive keratectomy (PRK). (Abstract). *Invest. Ophthalmol. Vis. Sci.* **37,** S18.

Science

In vivo confocal microscopy of the movement of microbeads through the aqueous outflow pathway

Arto Palkama[1], Roger W. Beuerman[2], Toshihiko Ohta[2],
Stephen C. Kaufman[2], Jeffrey A. Laird[2], & Herbert E. Kaufman[2]

[1]Department of Anatomy, University of Helsinki Medical School,
Helsinki, Finland
[2]Lions Eye Research Laboratories, LSU Eye Center,
Louisiana State University Medical Center School of Medicine,
2020 Gravier Street, Suite B,
New Orleans, Louisiana 70112-2234, USA
Correspondence should be addressed to R.W.B.

Correspondence to: Roger W. Beuerman, Ph.D., LSU Eye Center, 2020 Gravier Street, Suite B, New Orleans, LA 70112
Telephone: 504-568-6700, ext 331; Fax: 504-568-4210;
E-mail: rbeuer@lsumc.edu

Abstract

Glaucoma, a group of diseases characterized by increased fluid pressure within the eye, is a leading cause of blindness. Open-angle glaucoma, the most common form, involves impairment of a complicated outflow pathway comprising minute, highly specialized structures that regulate the movement of fluid from the anterior chamber of the eye through the aqueous plexus and into venous collecting channels. This study demonstrates the feasibility of using confocal microscopy to visualize the structures of the outflow pathway in the living mammalian eye. The velocity of microbeads was measured in the anterior chamber and the fluid- filled aqueous plexus; the reduced velocity in the anterior chamber suggests a resistance to flow, probably in the intervening trabecular meshwork. This new approach may be used to identify specific alterations in the outflow pathway in the living eye, leading to a new understanding of glaucoma and its treatment.

Glaucoma is a heterogeneous group of diseases, all of which lead to optic nerve damage and visual loss usually as a result of increased pressure in the eye caused by impaired fluid outflow[1]. The most prevalent type, primary open-angle glaucoma, is a leading cause of blindness throughout the world[1-4]. The prevalence of open-angle glaucoma was reported to be 6.3% in a group of elderly persons in California[4]. Another study showed that the prevalence varies from country to country in northern Europe[3]. Although the cause of this blinding eye disease remains unknown, the population at risk is growing, particularly with the aging of the "baby boomer" generation in the United States. It has been estimated that nearly 2.5 million persons in the U.S. will be afflicted with this disorder by the turn of the century[5].

In open-angle glaucoma, restriction of the outflow of aqueous humor from the interior of the eye to the venous drainage system is thought to involve impeded passage through a narrow cleft of loose fibrous tissue, the trabecular meshwork. Recently, a gene has been discovered that encodes a trabecular meshwork protein, and a mutation of this gene appears to be associated with patients who have primary open-angle glaucoma[6]. Possible causes of failure of outflow, and hence the damaging rise in intraocular pressure, include pathologic changes in the structure of the meshwork and/or obstruction of the aqueous pathway by collapse of the channels carrying fluid away from the meshwork[7-9]. It has also been suggested that not all cases of glaucoma are caused by the same mechanism. Diagnosis and determination of the prognosis for a given patient require intraocular pressure measurements, visual fields testing, and evaluation of the anterior chamber angle. Studies in rabbits and monkeys involving experimental manipulation of intraocular pressure are inconclusive in their elucidation of the outflow mechanisms[10,11]. To date, direct evaluation of the structures

of the aqueous outflow pathway at the cellular level has not been possible; with the new confocal microscopy methodology described in this study, such an approach may become practical and useful in both diagnosis and the determination of optimal therapy.

The white-light confocal microscope provides in vivo cellular level analysis of events such as fibroblast activation and epithelial wound healing. Confocal microscopic measurement and morphological characterization of cells in the living eye allow precise identification of phenotype for both tissue cells and cells of immune origin[7-9,12-14]. White-light confocal microscopy is non-destructive, permitting repeated in vivo observations of cellular processes, such as migration of inflammatory cells from the vascular space, fibroblastic activation of cells, and the response to chemical manipulation and disease processes, over time[15,16].

The outflow pathway in the rabbit has structural components analogous to those of the primate; fluid drains from the anterior chamber into a fibrous meshwork, thence into the aqueous plexus, and finally into venous collecting channels. The aqueous plexus -- Fontana's space in rabbits, Schlemm's canal in primates -- has been difficult to separate from the trabecular meshwork as a cause of increased intraocular pressure, because it has not been possible to directly observe changes in its dimensions or the through-flow into the aqueous drainage system in the living eye. In this study, we demonstrate that, with confocal microscopy, it is possible to observe microbeads injected into the anterior chamber of normal rabbit eyes moving in the anterior chamber and in the aqueous plexus. By measuring the differential velocity of flow in these structures, the presence of an intervening resistance, probably the fibrous trabecular meshwork, may be inferred.

Results

Rabbits were anesthetized and 9-0 sutures (30 μm diameter) were placed at the corneoscleral limbus (the junction between the cornea and the sclera) to identify the area during confocal microscopy. A 23-gauge needle with a constriction half way along its length and having small holes above and below the constriction was introduced transcorneally, avoiding contact with the iris (Fig. 1). One end of the needle was connected by polyethylene tubing to a 10-μl syringe and the other end to a reservoir containing Ringer's solution and a pressure transducer to prevent changes in intraocular pressure. Microbeads were injected into the anterior chamber slowly over 5 minutes. The objective of the confocal microscope was carefully brought into position. A thin layer of 10% methylcellulose was used as an optical coupler; there was no direct contact between the eye and the microscope. The three layers of the cornea (epithelium, stroma, and endothelium) were identified[7-9,12,13].

As the objective of the confocal microscope was moved across the corneal surface toward the periphery where the cornea meets the sclera, microbeads were observed in the aqueous humor just posterior to the endothelium (Fig. 2) and at the anterior surface of the iris (not depicted). The vessels of the conjunctiva and the flow of red blood cells and cells of immune origin were noted as the plane of focus moved downward at the corneoscleral limbus. Microbeads in the anterior chamber were recorded on video tape for up to 20 seconds. The mean velocity of the microbeads in the anterior chamber was determined to be 7.2 μm/sec $\pm$ 0.38 μm/sec (n=5).

Microbeads that had been injected into the anterior chamber were observed in vivo by confocal microscopy in the aqueous plexus (Fontana's space) (Fig. 3). The mean velocity of the microbeads in Fontana's space was found to be 64.3 μm/sec $\pm$ 3.1 μm/sec (n=5) (Fig.

3), which was significantly faster than the rate in the anterior chamber ($p > 0.01$). Confocal microscopy showed the opaque suture, which was approximately 30 μm in diameter, above Fontana's space; the diameter of Fontana's space varied from 30 to 50 μm. A venous collecting channel was seen to open directly into this space (Fig. 3). Histological analysis (Fig. 4) also identified the connection between the aqueous plexus and the venous collecting channels seen in vivo by confocal microscopy (Fig. 3). An accumulation of microbeads in Fontana's space was identified in frozen sections, and the variable diameter of this space previously measured by confocal microscopy was verified (Fig. 4). The appearance of these structures as seen by confocal microscopy, as well as our histological results, are corroborated by an earlier histological study of the rabbit outflow pathway[17].

Discussion

The clinical ability to visualize the outflow apparatus in the glaucomatous eye in humans may lead to increased understanding of the disease, the ability to diagnose the early signs of the disease, and based on the site of the outflow abnormality, the individualization of therapy to the specific type of glaucomatous pathology. Glaucoma is treated by several modalities, including drugs, laser surgery, and filtration surgery; the ability to visualize the outflow pathway provides a direct means of observing the therapeutic effects. Some of the mechanisms that cause various types of glaucoma, such as the elevated intraocular pressure induced by the therapeutic use of corticosteroids, may be different from the mechanism that causes primary open-angle glaucoma. Modification of this technique to improve our understanding of the dynamics of aqueous humor outflow in humans may lead to improved therapeutic measures. The ability to correlate structural changes in the trabecular meshwork

and Schlemm's canal in the living human eye with the type of glaucoma could provide new insights into this blinding eye disease.

Additionally, this new application of confocal microscopy, in conjunction with the appropriate tracers (or stains), will give us a unique new experimental tool to evaluate the flow of aqueous humor in glaucoma. For the first time, we can directly evaluate the rate of the movement of aqueous humor through the anterior chamber angle. This also provides a potentially powerful tool to evaluate the effect of new glaucoma drugs with respect to their ability to change the structural resistance (flow) of the components that make up the outflow pathway. In particular, confocal microscopy may be useful to better understand the contribution of uveoscleral outflow to the intraocular pressure regulation, which is not well understood[18,19].

Methods

Animal care and treatment in this investigation were in compliance with the ARVO Resolution on the Use of Animals in Research. New Zealand white rabbits (2-3 kg) were anesthetized by intramuscular injection of ketamine hydrochloride (30 mg/kg) and xylazine (6 mg/kg). A 6-0 suture to adjust eye position was attached to a superficial location approximately at the 12:00 o'clock position. The rabbits were wrapped in a pad to maintain body temperature and positioned on their side in a specially designed holder. The eyelids were held open by a wire speculum.

An aliquot of 7.4×10^5 microbeads/ml in water was diluted with sterile 0.9% NaCl, such that a 5-μl aliquot contained 3.7×10^4 microbeads. For each observation, a 5-μl aliquot was injected into the anterior chamber of the rabbit eye over a period of 5 minutes (Fig. 1).

The microbeads (Bangs Laboratories, Inc., Fishers, Indiana) were made of polystyrene without surface functional groups and contained a black organic nonpermeable material. The microbeads were 2.5 μm $\pm$ 10% in diameter, with a density of 1.05 g/ml.

For confocal microscopy, as in previous studies on humans and animals[14,16], the cornea was covered with an optically thin layer of 10% methylcellulose and the convex surface of the objective was brought into position. Images were viewed as the plane of focus was moved through the tissue in increments of a few microns, with the confocal microscopic images viewed in real-time on a video monitor (Sony Medical Monitor) and recorded through a CCD camera (Videoscope, Washington, DC) onto S-VHS tape for later playback and analysis[14-16].

To determine the average velocity of the microbeads in the anterior chamber and Fontana's space, individual frames were captured from S-VHS videotape every 0.2 seconds on an Epic 2MEG (Epic, Buffalo Grove, Illinois) frame grabber and transferred to Optimas software (Optimas Corp., Seattle, Washington). Pixel to micrometer conversion was made for the images. Instantaneous velocity for each time point was calculated by determining the change in position for each time point; mean velocity was calculated as the average of all of the instantaneous velocity calculations for each time and position.

At the conclusion of the experiment, the animals were killed by an overdose of sodium pentobarbital. The eye was initially fixed by immersion in a fixation solution, frozen, and prepared for cryostat sections (7 μm). Dark field microscopy and photography were performed using a Leica research microscope.

Acknowledgements

This work was supported by U.S. Public Health Service Grants EY04074, EY02580, and EY02377 from the National Eye Institute, National Institute of Health, Bethesda, Maryland; Department of the Army, Cooperative Agreement DAMD 17-93-V-3013 (This does not necessarily reflect the position or the policy of the government, and no official endorsement should be inferred.); and a departmental grant from Research to Prevent Blindness, Inc., New York, New York. Support from LSU Eye Center Visionary Gala is also acknowledged.

1. Tielsch, J.M. The epidemiology and control of open angle glaucoma: a population-based perspective. *Annu. Rev. Public Health* **17**, 121-136 (1996).

2. Nemesure, B., Leske, M.C., He, Q., & Mendell, N. Analysis of reported family history of glaucoma: a preliminary investigation. The Barbados Eye Study Group. *Ophthalmic Epidemiol.* **3**, 135-141 (1996).

3. Ringvold, A. Epidemiology of glaucoma in northern Europe. *Eur. J. Ophthalmol.* **6**, 26-29 (1996).

4. Dougherty, P.J., Engelhardt, R.F., & Lee, D.A. Eye disease among ambulatory Jewish senior citizens in California. *J. Community Health* **19**, 271-284 (1994).

5. Quigley, H.A. & Vitale, S. Models of open-angle glaucoma prevalence and incidence in the United States. *Invest. Ophthalmol. Vis. Sci.* **38**, 83-91 (1997).

6. Stone, E.M. *et al.* Identification of a gene that causes primary open angle glaucoma. *Science* **275**, 668-670 (1997).

7. Ten Hulzen, R.D. & Johnson, D.H. Effect of fixation pressure on juxtacanalicular tissue and Schlemm's canal. *Invest. Ophthalmol. Vis. Sci.* **37**, 114-124 (1996).

8. Allingham, R.R., de Kater, A.W., & Ethier, C.R. Schlemm's canal and primary open angle glaucoma: correlation between Schlemm's canal dimensions and outflow facility. *Exp. Eye Res.* **62**, 101-109 (1996).

9. Grierson, I., Nagasubramanian, S., Edwards, J., Miller, L.C., & Ennis, K. The effects of various levels of intraocular pressure on the rabbit's outflow system. *Exp. Eye Res.* **42**, 383-397 (1986).

10. Tingey, D.P., Schroeder, A., Epstein, M.P., & Epstein, D.L. Effects of topical ethacrynic acid adducts on intraocular pressure in rabbits and monkeys. *Arch.*

Ophthalmol. **110**, 699-702 (1992).

11. Finger, P.T., Moshfeghi, D.M., Smith, P.D., & Perry, H.D. Microwave cyclodestruction for glaucoma in a rabbit model. *Arch. Ophthalmol.* **109**, 1001-1004 (1991).

12. Chew, S.J., Beuerman, R.W., & Kaufman, H.E. Real-time confocal microscopy of keratocyte activity in wound healing after cryoablation in rabbit corneas. *Scanning* **16**, 269-274 (1994).

13. Chew, S.J. *et al.* Early diagnosis of infectious keratitis with in vivo real time confocal microscopy. *CLAO J.* **18**, 197-201 (1992).

14. Beuerman, R.W., Laird, J.A., Kaufman, S.C. & Kaufman, H.E. Quantification of real-time confocal images of the human cornea. *J. Neurosci. Meth.* **54**, 197-203 (1994).

15. Cohen, R.A. *et al.* Confocal microscopy of corneal graft rejection. *Cornea* **14**, 467-472 (1995).

16. Kaufman, S.C., Laird, J.A., Cooper, R. & Beuerman, R.W. Diagnosis of bacterial contact lens-related keratitis with the white-light confocal microscope. *CLAO J* **22**. 274-277 (1996).

17. Knepper, P.A., McLone, D.G., Goossens, W., Vanden Hoek, T., & Higbee, R.G Ultrastructural alterations in the aqueous outflow pathway of buphthalmic rabbits. *Exp. Eye Res.* **52**, 525-533 (1991).

18. Poyer, J.F., Gabelt, B., & Kaufman, P.L. The effect of topical $PGF_{2\alpha}$ on uveoscleral outflow and outflow facility in the rabbit eye. *Exp. Eye Res.* **54**, 277-283 (1992)

19. Camras, C.B., Bito, L.Z., & Eakins, K.E. Reduction of intraocular pressure by

prostaglandins applied topically to the eyes of conscious rabbits. *Invest. Ophthalmol. Vis. Sci.* **16**, 1125-1134 (1977).

Figure Legends

Fig. 1 Schematic diagram of ocular preparation for confocal microscopy of microbead movement through the anterior chamber and aqueous plexus. A needle inserted across a corneal diameter allowed measurement of the intraocular pressure during the injection of a 5-μl aliquot of a sodium chloride solution containing the microbeads. Intraocular pressure was held constant by the saline column. The objective of the confocal microscope was moved around to visualize the aqueous outflow pathway. The layer of methylcellulose used as an optical coupler is indicated by the lined segment between the objective of the confocal microscope and the corneal surface; the thickness of the layer is exaggerated for visibility.

Fig. 2 Confocal micrograph of microbeads in the anterior chamber. The corneal endothelial cells (E) can be seen in outline. To view both the central and peripheral areas of the anterior chamber, the objective was moved over the corneal surface with adjustments for changes in corneal thickness. The outflow meshwork (not shown) was identified by its loose fibrous structure.

Fig. 3 Confocal micrographs of the movement of a single microbead in the fluid-filled space of Fontana. (A) This view shows bead movement beginning at an arbitrary time and location denoted by the parallel solid white lines. (B) The time is 1.5 sec after the view in (A), and the bead has moved 70.2 μm, giving a velocity of 83.8 μm/sec. (C) The bead has moved an additional 87.2 μm, giving a velocity of 81.2 μm/sec. A venous collecting channel (CC) and its opening into the space are visible in all three views. Compare the view

in (C) with Figure 4. S, Fontana's space. Bar, 75 μm.

Fig. 4 Seven-micron-thick cryostat sections of the anterior chamber angle of the rabbit eye depicting the fluid and flow structures. Top. Two collecting channels (CC) are seen to course outward from areas of the plexus close to Fontana's space (S). Note the ciliary processes (CP) at the bottom of the figure. The junction of the cornea (on the left) with the sclera (on the right), known as the corneoscleral limbus, is defined by the termination of Descemet's layer (D), which underlies only the cornea and does not extend beneath the sclera. AC, anterior chamber. (Magnification, x 130). Bottom. In a higher magnification, the microbeads are visible just below Descemet's layer (D) and in Fontana's space (S), and the tubular nature of the collecting channels (CC) can be seen. D, Descemet's membrane. (Magnification, x 328).